

Accepted Manuscript

6-Aryl substituted 4-(4-cyanomethyl) phenylamino quinazolines as a new class of isoform-selective PI3K-alpha inhibitors

Rammohan R. Yadav, Santosh K. Guru, Prashant Joshi, Girish Mahajan, Mubashir J. Minto, Vikas Kumar, Sonali S. Bharate, Dilip M. Mondhe, Ram A. Vishwakarma, Shashi Bhushan, Sandip B. Bharate

PII: S0223-5234(16)30553-0

DOI: [10.1016/j.ejmech.2016.07.006](https://doi.org/10.1016/j.ejmech.2016.07.006)

Reference: EJMECH 8724

To appear in: *European Journal of Medicinal Chemistry*

Received Date: 28 April 2016

Revised Date: 4 July 2016

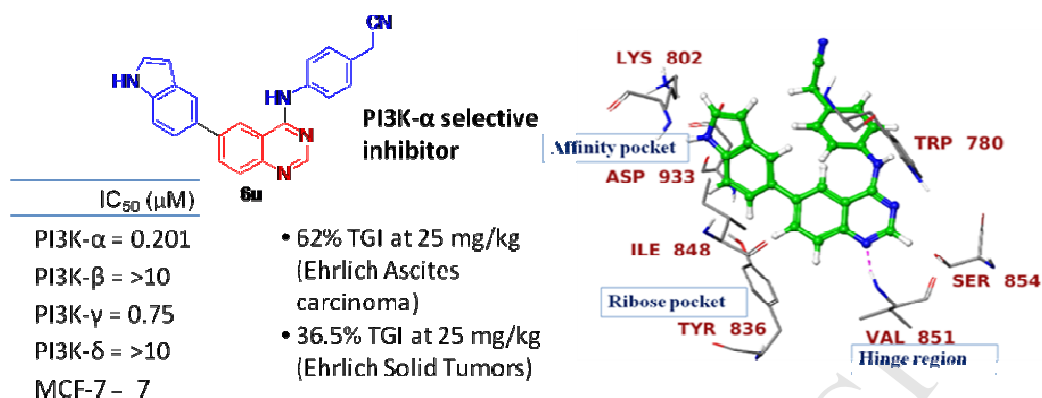
Accepted Date: 5 July 2016

Please cite this article as: R.R. Yadav, S.K. Guru, P. Joshi, G. Mahajan, M.J. Minto, V. Kumar, S.S. Bharate, D.M. Mondhe, R.A. Vishwakarma, S. Bhushan, S.B. Bharate, 6-Aryl substituted 4-(4-cyanomethyl) phenylamino quinazolines as a new class of isoform-selective PI3K-alpha inhibitors, *European Journal of Medicinal Chemistry* (2016), doi: 10.1016/j.ejmech.2016.07.006.

This is a PDF file of an unedited manuscript that has been accepted for publication. As a service to our customers we are providing this early version of the manuscript. The manuscript will undergo copyediting, typesetting, and review of the resulting proof before it is published in its final form. Please note that during the production process errors may be discovered which could affect the content, and all legal disclaimers that apply to the journal pertain.



GRAPHICAL ABSTRACT



An isoform-selective quinazoline class of PI3K- α inhibitor possessing in-vitro and in-vivo anticancer activity has been identified.

6-Aryl substituted 4-(4-cyanomethyl) phenylamino quinazolines as a new class of isoform-selective PI3K-alpha inhibitors

Rammohan R. Yadav,^{a,b#} Santosh K. Guru,^{c#} Prashant Joshi,^{a,b} Girish Mahajan,^{b,c} Mubashir J. Minto,^{b,c} Vikas Kumar,^{b,d} Sonali S. Bharate,^d Dilip M. Mondhe,^{b,c} Ram A. Vishwakarma,^{a,b} Shashi Bhushan*^{b,c} and Sandip B. Bharate^{a,b,*}

^a*Medicinal Chemistry Division, CSIR-Indian Institute of Integrative Medicine, Canal Road, Jammu-180001, India.*

^b*Academy of Scientific & Innovative Research (AcSIR), CSIR-Indian Institute of Integrative Medicine, Canal Road, Jammu-180001, India*

^c*Cancer Pharmacology Division, CSIR-Indian Institute of Integrative Medicine, Canal Road, Jammu-180001, India. *E-mail:*

^d*Preformulation Laboratory, PKPD Division, CSIR-Indian Institute of Integrative Medicine, Canal Road, Jammu-180001, India*

**Corresponding authors. E-mail: sbharate@iiim.ac.in (SBB); sbhushan@iiim.ac.in (SB); Fax: +91-191-2585333; Tel: +91-191-2585006*

ABSTRACT:

Isoform-selective inhibition of PI3K- α has been identified as one of the important strategy to discover effective and safer anticancer agents. Herein, we report discovery of 'quinazoline' as a new chemotype for isoform-selective PI3K- α inhibitors. The indolyl substituted quinazoline **9u**

displayed selective inhibition of PI3K- α with IC_{50} value of 0.201 μ M with >49.7 over PI3K- β , and δ -isoforms. Quinazoline **9u** also inhibited PI3K- γ with IC_{50} value of 0.750 μ M (3.7 fold selective for α - versus γ -isoform). The isoform-selective inhibition was also demonstrated at protein-expression level by western-blot analysis in MCF-7 and PC-3 cells. The isoform-selective inhibitor **9u** also showed inhibition of phospho-Akt levels in these cells. Quinazoline **9u** showed promising cytotoxicity in MCF-7 cells with GI_{50} of 7 μ M, which was highly selective for cancer cells, as it was non-toxic to normal cells fR2, HEK293 and hGF ($GI_{50} > 50 \mu$ M). Compound **9u** at 25 mg/kg dose showed 62 and 37% TGI in Ehrlich Ascites Carcinoma and Ehrlich Solid Tumor mice models. In nutshell, our efforts to identify potent and efficacious PI3K inhibitors resulted in the discovery of a new class of isoform-selective PI3K- α inhibitors possessing promising *in-vivo* anticancer activity.

KEYWORDS:

6-aryl quinazolines, isoform-selective, PI3K-alpha, breast cancer, anticancer agents

1. INTRODUCTION

The PI3K signalling pathway coordinates large number of physiological functions in humans including cell growth, proliferation, metabolism, survival and motility [1-4]. Biochemical studies in large number of tumour tissues revealed that PI3K signalling cascade is dysregulated in breast, colon, endometrial, brain and prostate cancers. PI3K signalling genes PIK3CA, PIK3CB, PIK3CD and PIK3CG encodes different PI3K isoforms (PI3K- α , β , δ and γ). Several studies have demonstrated that PI3K- α isoform plays crucial role in cancer progression, due to the mutation or amplification of the PIK3CA gene or increased expression of P110 α in most of the tumor types, whereas PI3K- β isoform is involved in PTEN deficient tumors. However, both PIK3CA mutation as well as PTEN deficiency is not common in PI3K- δ associated tumors [4-6]. The early discovery of pan-PI3K inhibitors wortmannin [7] and LY294002 [8] and GDC-0941 [9, 10] were critical events that allowed rapid exploration of PI3K signalling, which led to their extensive usage as a tool compounds against a variety human tumour histotypes *in-vitro* and *in-vivo*. Later, with the discovery of mTOR as a molecular target of rapamycin, numerous dual PI3K/mTOR inhibitors were discovered; and many of them reached to clinical stages, including NVP-BEZ235 (**1**) [11-13]. The pan-PI3K inhibitors and dual PI3K/mTOR inhibitors faced problems in clinical trials, with limited efficacies as a monotherapeutic agent as well as a relatively high rate of side effects, because of their off-target activity [2, 6, 13-15]. Thus, the discovery of isoform-selective PI3K kinase inhibitors has always remained a priority of medicinal chemists in order to improve efficacy while minimizing undesirable side effects.

The success of PI3K isoform-selective inhibitors has been demonstrated by idelalisib (CAL101, **2**), a first-in-class PI3K δ -selective small-molecule inhibitor that has been approved by the FDA for the treatment of chronic lymphocytic leukemia, relapsed small lymphocytic

lymphoma and B-cell non-Hodgkin's lymphoma [16]. Furthermore, more than a dozen isoform-selective PI3K inhibitors are in various stages of clinical trials. Some of them includes NVP-BYL719 (**3**) [17, 18], GDC-0032 (**4**) [19, 20] and INK1117 (**5**) [21] for PI3K- α , and AZD8186 (**6**) [22] and AZD-6482 (**7**) [23] for PI3K- β . The clinical success of isoform-selective PI3K inhibitor idelalisib, a quinazoline class of compound has motivated us to look for isoform-selective inhibitors from this scaffold. A pan-PI3K inhibitor BAY 80-6946 (**8**) [24] is reported from this scaffold, however a PI3K- α selective inhibitor has never been reported.

Amongst all four isoforms of PI3K, the importance and high frequency of PIK3CA mutation in most of the solid tumors has attracted attention towards the development of PI3K α -selective inhibitors. The aim of present work was to design, synthesize and optimize quinazoline scaffold for selective binding to PI3K- α ATP binding site. A series of 6-aryl quinazolines **9a-x** were prepared and screened for PI3K- α / mTOR inhibitory activity and cytotoxicity in a panel of cancer cell lines; and the best compounds were investigated for their *in-vivo* anticancer activity in murine tumor models.

<< Figure 1 >>

2. RESULTS AND DISCUSSION

2.1. Design. The close analysis of PI3K- α ATP binding site reveals the presence of a small polypeptide chain (a hinge region) connecting the C-lobe and N-lobe of PI3K, which interacts with adenine part of ATP. Literature precedence suggests that diverse fragments such as quinazoline (idelalisib), quinoline (GSK2126458 [25] and PF-04979064 [26]), 2-aminothiazole (NVP-BYL719 and PIK-93) [17] and morpholine group (PI-103 and GDC-0914) [9] interact with the hinge region. Herein, we chose quinazoline as a key hinge binding pharmacophore in

the designed compounds, wherein the “N=CH-N” fragment interacts with the Val851 of hinge region (Figure 1B).

The chemical association of hinge binding functionality with the aromatic and heteroaromatic rings increases the potency drastically as seen in the case of NVP-BEZ235, NVP-BYL719, GSK2126458 and PF-04979064. Therefore, C6-substitution on quinazoline with heteroaromatic rings was selected in order to maintain interactions in the affinity pocket. Another common feature in pan-PI3K inhibitors and isoform-selective PI3K- α inhibitors is their ATP-competitive inhibition *via* blockage of substrate lipid phosphorylation, however, interactions with the un-conserved residues in ATP binding site and solvent exposed area, has been reported to provide isoform-selectivity. Docking studies of NVP-BEZ235 and NVP-BYL719 indicated that introduction of 4-(4-cyanomethyl)phenylamino functionality at C-4 position led to interactions of designed analogs with un-conserved residues. Therefore, this functionality was incorporated in designed compounds (as shown in Figure 1B).

2.2. Synthesis. The synthetic scheme for preparation of quinazolines **9a-x** is depicted in Scheme 1. The first step involves treatment of anthranilic acid (**10**) with bromine in acetic acid to produce 2-amino-5-bromobenzoic acid **11** in 55% yield [27]. Further, the treatment of 2-amino-5-bromobenzoic acid (**11**) with formamide resulted in formation of 4-hydroxy quinazoline (**12**) in 72% yield. Treatment of 4-hydroxy quinazoline (**12**) with phosphorous oxychloride resulted in formation of 4-chloro 6-bromoquinazoline **13** in 92% yield [28]. The intermediate **13** was then treated with 4-amino benzylcyanide (**14**) to get a key intermediate (**15**) required for Suzuki coupling reaction [29]. Finally, Suzuki-Miyaura coupling of intermediate **15** with various aryl and heteroaryl boronic acids using tetrakis(triphenylphosphine)palladium catalyst produced 6-aryl substituted 4-(4-cyanomethyl) phenylamino quinazolines **9a-x** in 43-81% yield. The 6,7-

dimethoxy 4-(4-cyanomethyl) phenylamino quinazoline **19** was also synthesized using similar synthetic strategy as depicted in Scheme 1.

<< Scheme 1 >>

2.3. In-vitro screening for PI3K inhibition and cytotoxicity and isoform-selectivity. All synthesized 6-substituted quinazolines were first tested for inhibition of PI3K- α and mTOR at 0.5-1 μ M. Amongst all tested compounds, analogs **9e**, **9p**, **9u**, **9w** and **9x** were the potent inhibitors of PI3K- α showing 70, 48.6, 47.5, 45.6 and 49% inhibition at 0.5 μ M. Other analogs with >30% inhibition of PI3K- α were **9a**, **9d**, **9f**, **9h**, and **9o**. Further, the IC₅₀ was determined for best 10 analogs for PI3K- α inhibition and results are shown in Table 1. Analog **9e**, **9u** and **9x** were found to inhibit PI3K- α with IC₅₀ values of 115, 201 and 150 nM, respectively. None of the compound showed inhibition of mTOR at a tested concentration (1 μ M).

<< Table 1 >>

The analysis of PI3K- α crystal structures and function reveals that all known PI3K inhibitors interacts with the common hinge binding region Val851 residue by H-bonding and mimic the adenine part of ATP, which consequently inhibit substrate phosphorylation. However, further extension and interaction of inhibitor structural features in the affinity pocket, and solvent exposed area defines the enzyme inhibition potency. As anticipated, molecular docking of **9u** and **9x** with PI3K- α ATP binding site (using PDB: 4L23) considering PI-103 as centroid of docking grid reveals that quinazoline core interacts with the Val851 residue backbone in hinge pocket by H-bonding and mimic the adenine ring of ATP. The bisaromatic heterocyclic core interacts with the Tyr836 residue of ribose pocket by aromatic π - π stacking. H-bonding and π - π stacking at hinge pocket stabilize the conformation of ligands in such a way that it extends its 6-heteroaryl ring i.e. indolyl and quinolinyl group towards the affinity pocket Lys802 and Asp933

through bypassing the gatekeeper Ile848 residue which physically block entry of donor substrate ATP as displayed in Figure 2.

<< Figure 2 >>

Next, we studied selected 10 best compounds for their isoform-selectivity against other PI3K isoforms. Amongst tested compounds, indolyl substituted analog **9u** displayed promising selectivity towards PI3K- α isoform over β - and δ -isoforms (>49 fold selectivity). The isoquinolinyl substituted analog **9x** displayed high selectivity towards PI3K- α isoform over β - and γ -isoform (\geq 56-fold selectivity). In particular, the compound **9x** did not inhibit (0% inhibition) PI3K- β up to 20 μ M. Thus, the compound **9u** is a selective dual alpha/gamma inhibitor with a slight preference for alpha; whereas compound **9x** is a selective dual alpha/delta inhibitor with a slight preference for alpha.

4-Acetylphenyl substituted analog **9d** was found to be an inhibitor of PI3K- α and γ isoforms with IC_{50} values of 270 and 150 nM, respectively. Interestingly, 4-vinylphenyl substituted analog **9h** was found to be a selective inhibitor of PI3K- γ , and with no inhibition of PI3K- α , β and δ isoforms (IC_{50} >10 μ M). PI3K family member kinases share close homology in structural sequence, function and topology and therefore, targeting of cancer cells by isoform-selective PI3K inhibitors is challenging due to conserved kinase residues (PI3K- α and γ share ~35% overall homology and ~43.5% kinase domain) [30] in ATP binding site.

Experimentally, it was observed that **9u** inhibit both α and γ isoforms with moderate selectivity (4-fold selective towards PI3K- α), however, **9x** selectively inhibit PI3K- α enzyme over PI3K- γ (>50-fold selective). Comparison of interactions of **9x** with PI3K- α (PDB: 4L23) and PI3K- γ isoform (PDB: 3IBE) reveals that at selectivity pocket/activation loop of enzymes, benzyl

cyanide group adopts different conformations due to difference in topology of PI3K- α and PI3K- γ isoform. Furthermore, in PI3K- γ solvent exposed area, neutral Gln859, Ser854, and Ser 919 residues of PI3K- α were replaced by the charged Lys890, Ala885, and Asp950 residues, which leads to loss of vander waal interactions as shown in supporting information (Figure S1).

All compounds were then screened for cytotoxicity in a panel of cancer lines including HL-60 (human leukemia cells), A-375 (human malignant melanoma), MCF-7 (human breast adenocarcinoma cell line), Panc-1 (human pancreatic cancer), and PC-3 (human prostate cancer) using 48 h as incubation time. Results are depicted in Table 2. The 6-isoquinolinyll derivative **9x** displayed significant cytotoxicity in all tested cancer lines with GI₅₀ values in the range of 9-12 μ M. Compound **9x** displayed time-dependent cytotoxicity in PC-3 cells, possessing GI₅₀ of 567, 189, 28 and 9 μ M at 6, 12, 24 and 48 h, respectively. The 6-indolyl substituted derivative **9u** showed promising *in-vitro* cytotoxicity in breast cancer MCF-7 cells with GI₅₀ value of 7 μ M. The 6-(2,4-difluorophenyl) substituted analog **9b** showed significant cytotoxicity in HL-60 and A375 cells with GI₅₀ values of 7 and 9 μ M, respectively. Two best compounds **9u** and **9x** were then screened for *in-vitro* cytotoxicity in 3 normal cell lines (Table 3). Results indicated that these compound are non-toxic to normals cells (GI₅₀ >50 μ M). In order to address the cell death caused by compounds **9u** and **9x**, the extent of apoptotic death in MCF-7 and PC-3 cell lines was assessed using flow cytometry and by analyzing effect on mitochondrial membrane potential (MMP) loss. Both compounds exhibited a dose-dependent increase in sub-G1 population (apoptosis), and also showed mitochondrial membrane potential (MMP) loss in MCF-7 and PC-3 cells (see, Figure S2 and S3 of supporting information).

<< Table 2 >>

<< Table 3 >>

To assess the obtained isoform-selectivity results of enzyme assays, the effect of compounds **9u** and **9x** on the expression of various isoforms of PI3K (α , β , γ and δ) was investigated in MCF-7 and PC-3 cells by western-blot analysis. As seen in Figure 3a, compound **9u** showed 44, 4, 16 and 30% inhibition of PI3K- α , β , γ and δ isoforms at 30 μ M in MCF-7 cells, indicating selectivity towards α -isoform. Similarly, another compound **9x** also displayed higher selectivity towards α -isoform over other three isoforms. As seen in Figure 3b, compound **9x** showed 100, 42, 20 and 32% inhibition of PI3K- α , β , γ and δ isoforms at 30 μ M in PC-3 cells, respectively (Figure 3a-d).

The PI3K activation phosphorylates and activates Akt in the plasma membrane. Activated Akt mediates downstream responses, including cell survival, growth, proliferation, cell migration and angiogenesis, by phosphorylating a range of intracellular proteins [31-33]. Therefore, the downstream effect of PI3K inhibition was assessed by investigating effect of these compounds on levels of phospho-Akt. Compounds **9u** and **9x** displayed 80% and 50% inhibition of phospho-Akt levels at 30 μ M, in MCF-7 and PC-3 cells, respectively (Figure 3a-d).

<< Figure 3 >>

2.4. Solubility, Caco-2 permeability, CYP liability and in-vivo anticancer activity. The solubility of most potent compounds **9e**, **9u** and **9x** was determined in water, PBS, SGF and SIF. All three compounds displayed good solubility in SGF (80-125 μ g/ml), whereas low solubility in water, PBS and SIF (1-10 μ g/ml) (Table S1 of supporting information). Compound **9x** does not have CYP liability against major metabolizing enzymes CYP3A4 and CYP2D6 (27 and 0% inhibition at 10 μ M). Similarly, another compound **9u** also do not have CYP liability (51 and 29 inhibition at 10 μ M) for these two major CYPs. Further, in Caco-2 permeability assay, the efflux

ratio of 1.2 and 1.3, indicated that these compounds are not substrates of efflux transporter pumps. Next, in order to demonstrate the anticancer activity in *in-vivo* models, these two compounds were tested for tumor growth inhibition in Ehrlich Ascites Carcinoma (EAC) model. EAC has undifferentiated cells and has a rapid growth rate and thus it resembles human tumors which are most sensitive to chemotherapy. The effect of compound treatment on the body weight of mice is shown in Table S2, which indicated that both these compounds does not led to change in body weight of animals. The tumor growth inhibition results of EAC cells are shown in Table 4. Compound **9x** showed 25.8% inhibition in the growth of EAC cells in the peritoneal cavity of experimental animals at a dose of 70 mg/kg of body weight. While, compound **9u** displayed promising tumor growth inhibition (62%) at 25 mg/kg dose. Based on the results obtained in EAC study, compound **9u** was further studied for its effect in Ehrlich Solid Tumor (EST) model, wherein it showed 36.5% TGI at 25 mg/kg dose without causing any mortality and change in body weight.

<< Table 4 >>

3. CONCLUSION

In summary, a series of 6-aryl substituted 4-(4-cyanomethyl)phenylamino quinazolines have been identified as a new class of potent and selective PI3K- α inhibitors. The 6-indolyl substituted quinazoline **9u** showed promising PI3K- α inhibition activity with excellent fold selectivity towards α -isoform with respect to PI3K β and PI3K- δ isoforms and moderate selectivity over PI3K- γ isoforms in both cell-free enzymatic and cell-based gene expression assay. The drug-like properties (no CYP/ efflux pump liability) and promising *in-vivo* tumor growth inhibition in

solid tumor model, indicated that compound **9u** has a promise for development as an anticancer agent.

4. EXPERIMENTAL SECTION

4.1. General. All chemicals were obtained from Sigma-Aldrich Company and used as received. ^1H , ^{13}C and DEPT NMR spectra were recorded on Bruker-Avance DPX FT-NMR 500 and 400 MHz instruments. Chemical data for protons are reported in parts per million (ppm) downfield from tetramethylsilane and are referenced to the residual proton in the NMR solvent (CDCl_3 , 7.26 ppm; CD_3OD , 3.31 ppm; $\text{DMSO-}d_6$, 2.50 ppm). The carbon nuclear magnetic resonance spectra (^{13}C NMR) were recorded at 125 MHz or 100 MHz; chemical data for carbons are reported in parts per million (ppm, δ scale) downfield from tetramethylsilane and are referenced to the carbon resonance of the solvent (CDCl_3 , 77.16 ppm; CD_3OD , 49.0 ppm; $\text{DMSO-}d_6$, 39.52 ppm). HR-ESIMS spectra were recorded on Agilent HR-ESIMS-6540-UHD machine. IR spectra were recorded on Perkin-Elmer IR spectrophotometer. Melting points were recorded on digital melting point apparatus. HPLC analysis was done on Shimadzu HPLC system (model: Shimadzu-LC 10AT) equipped with a PDA detector using Inertsil RP-18 (E-Merck, 5 μM , 4.0 x 250 mm) column and mobile phase used was acetonitrile and water as gradient at the flow rate of 0.8 ml/min. All kinase screening was done at International Center for Kinase profiling (ICKP), University of Dundee UK. The animals used in the study were bred in-house and used. The animal facility is registered with CPCSEA vide registration no. 67/99/CPCSEA. All of the biologically tested compounds have met the purity requirement.

4.2. Synthesis of 2-amino-5-bromobenzoic acid (11). The solution of anthranilic acid (**10**, 1 g, 7.3 mmol) in glacial acetic acid (10 mL) was cooled to 15 °C. Bromine solution (0.45 mL, 8.76 mmol) was added dropwise to the reaction mixture, which resulted in thick mass of white

glistening crystals consisting of the hydrobromides of the mono and dibromo anthranilic acid. The product was filtered off, washed with benzene and dried. It was then refluxed with dilute hydrochloric acid (20 mL) and filtered while hot under suction. The insoluble residue was extracted twice with boiling water (500 ml). The filtrate, upon cooling yielded an abundant precipitate of 2-amino-5-bromobenzoic acid (**11**). Yield: 55%; light brown solid; m.p. 209-211 °C; ^1H NMR (CD_3OD , 500 MHz): δ 7.87 (t, 1H, $J = 5.2$ Hz), 7.31-7.28 (m, 1H), 6.67 (dd, 1H, $J = 8.8, 5.2$ Hz); IR (CHCl_3): ν_{max} 3474, 3360, 2919, 1674, 1608, 1581, 1548, 1481, 1421, 1311, 1293, 1168, 1127, 1089, 1019 cm^{-1} ; HR-ESIMS: m/z 215.9654 calcd for $\text{C}_7\text{H}_6\text{BrNO}_2 + \text{H}^+$ (215.9655).

4.3. Synthesis of 6-bromoquinazolin-4-ol (12) and 6,7-dimethoxyquinazolin-4-ol (17). To the solution of 2-amino-5-bromo-benzoic acid (**11**, 1 g, 4.63 mmol) or 2-amino-4,5-dimethoxybenzoic acid (**16**, 1 g, 5.08 mmol), formamide (0.74 mL, 18.52 mmol for **11** and 0.8 mL, 20.3 mmol for **16**) was added and the resultant mixture was allowed to reflux at 150 °C for 6 h. After completion of reaction, the reaction mixture was filtered through Whatmann filter paper and dried under vacuum to get desired products **12** or **17**.

4.3.1. 6-Bromoquinazolin-4-ol (12): Yield: 70%; white solid; m.p. 273-275 °C; ^1H NMR ($\text{DMSO}-d_6$, 500 MHz): δ 8.20-8.16 (m, 1H), 7.98-7.95 (m, 1H), 7.63 (d, 1H, $J = 8.7$ Hz); IR (CHCl_3): ν_{max} 3442, 2922, 2852, 1726, 1697, 1605, 1465, 1389, 1318, 1272, 1239, 1220, 1178, 1019 cm^{-1} ; HR-ESIMS: m/z 226.9633 calcd for $\text{C}_8\text{H}_5^{81}\text{BrN}_2\text{O} + \text{H}^+$ (226.9658).

4.3.2. 6,7-Dimethoxyquinazolin-4-ol (17): Yield: 76%; white solid; m.p. 296-298 °C; ^1H NMR ($\text{DMSO}-d_6$, 400 MHz): δ 7.99 (s, 1H), 7.44 (s, 1H), 7.13 (s, 1H), 3.90 (s, 3H), 3.87 (s, 3H); IR (CHCl_3): ν_{max} 3416, 2919, 1649, 1606, 1505, 1438, 1402, 1356, 1307, 1287, 1270, 1247, 1212, 1125, 1074, 1025 cm^{-1} ; HR-ESIMS: m/z 207.0766 calcd for $\text{C}_{10}\text{H}_{10}\text{N}_2\text{O}_3 + \text{H}^+$ (207.0764).

4.4. Synthesis of 6-bromo-4-chloroquinazoline (13) and 4-chloro-6,7-dimethoxyquinazoline (18). The solution of 6-bromoquinazolin-4-ol (**12**, 1 g, 4.44 mmol) or 6,7-dimethoxyquinazolin-4-ol (**17**, 1 g, 4.13 mmol) in phosphorous oxychloride (5 mL) was refluxed for 6 h at 120 °C. The mixture was cooled to room temperature and poured into ice-water containing sodium bicarbonate to quench phosphorous oxychloride. The mixture was extracted with dichloromethane (3 × 100 ml) and the solvent was evaporated to get chlorinated products **13** or **18**.

4.4.1. 6-Bromo-4-chloroquinazoline (13): Yield: 74%; light yellow solid; m.p. 161-163 °C; ¹H NMR (CDCl₃, 500 MHz): δ 9.07 (s, 1H), 8.44 (d, 1H, *J* = 2.0 Hz), 8.05 (dd, 1H, *J* = 8.9, 2.2 Hz), 7.96 (d, 1H, *J* = 8.9 Hz); IR (CHCl₃): ν_{max} 2922, 1632, 1559, 1546, 1474, 1461, 1388, 1360, 1241, 1160, 1019 cm⁻¹; HR-ESIMS: *m/z* 242.9326 calcd for C₈H₄BrClN₂+H⁺ (242.9319).

4.4.2. 4-Chloro-6,7-dimethoxyquinazoline (18): Yield: 82%; light yellow solid; m.p. 184-186 °C; ¹H NMR (CDCl₃, 400 MHz): δ 8.88 (s, 1H), 7.40 (s, 1H), 7.34 (s, 1H), 4.09 (s, 6H); IR (CHCl₃): ν_{max} 1674, 1614, 1557, 1510, 1473, 1455, 1442, 1435, 1413, 1357, 1349, 1281, 1259, 1204, 1164, 1124, 1071, 1029, 1013 cm⁻¹; HR-ESIMS: *m/z* 225.0428 calcd for C₁₀H₉ClN₂O₂+H⁺ (225.0425).

4.5. Synthesis of 6-bromo-4-(4-cyanomethyl)phenylamino quinazoline (15) and 6,7-dimethoxy-4-(4-cyanomethyl)phenylamino quinazoline (19). The mixture of 6-bromo-4-chloroquinazoline (**13**, 0.2 g, 0.83 mmol) or 4-chloro-6,7-dimethoxyquinazoline (**18**, 0.2 g, 0.89 mmol) and 4-amino benzyl cyanide (**14**, 0.142 g, 1.07 mmol for **13** and 0.153 g, 1.16 mmol for **18**) in isopropanol (5 mL) was allowed to stir for 3 h under reflux condition. After completion of reaction, the mixture was filtered through Whatman filter paper and dried under vacuum to get the desired products **15** or **19**.

4.5.1. *6-Bromo-4-(4-cyanomethyl)phenylamino quinazoline (15)*: Yield: 82%; brown solid; m.p. 275-277 °C; ^1H NMR (DMSO- d_6 , 400 MHz): δ 9.20 (s, 1H), 8.93 (s, 1H), 8.30-8.23 (m, 1H), 7.96-7.89 (m, 1H), 7.83-7.76 (m, 2H), 7.48 (d, 2H, $J = 7.2$ Hz), 4.10 (s, 2H); ^{13}C NMR (DMSO- d_6 , 100 MHz): δ 158.71, 151.16, 138.71, 138.18, 135.91, 129.56, 128.43, 127.17, 124.96, 122.15, 120.86, 119.05, 115.01, 21.98; IR (CHCl₃): ν_{max} 3437, 2922, 1649, 1621, 1594, 1545, 1464, 1406, 1273, 1098, 1018 cm^{-1} ; HR-ESIMS: m/z 339.0243 calcd for C₁₆H₁₁BrN₄+H⁺ (339.0240).

4.5.2. *6,7-Dimethoxy-4-(4-cyanomethyl)phenylamino quinazoline (19)*: Yield: 72%; brown solid; m.p. 268-270 °C; HPLC purity: 99% ($t_{\text{R}} = 24.58$ min); ^1H NMR (DMSO- d_6 , 400 MHz): δ 11.40 (s, 1H), 8.82 (s, 1H), 8.31 (s, 1H), 7.72 (d, 2H, $J = 8.4$ Hz), 7.47 (d, 2H, $J = 8.4$ Hz), 7.35 (s, 1H), 4.10 (s, 2H), 4.02 (s, 3H), 4.0 (s, 3H); ^{13}C NMR (Pyridine- d_5 + D₂O, 100 MHz): δ 159.45, 157.24, 155.19, 151.90, 148.72, 141.53, 130.70, 128.24, 121.57, 111.88, 108.97, 104.32, 58.68, 58.25, 24.69; IR (CHCl₃): ν_{max} 3369, 2953, 2921, 2852, 1738, 1628, 1508, 1575, 1453, 1402, 1363, 1320, 1152, 1065, 1018 cm^{-1} ; HR-ESIMS: m/z 321.1348 calcd for C₁₈H₁₆N₄O₂+H⁺ (321.1346).

4.6. Procedure for Suzuki coupling: Synthesis of compounds 9a-x. A solution of 2M K₂CO₃ solution (3 ml) in dioxane (3 ml) was taken in round bottom flask and was purged with nitrogen balloon for 5 min at room temperature. A mixture of boronic acid (1.2 mmol) and compound **15** (0.1 g, 1 mmol) was added to this reaction mixture, and it was again purged with nitrogen for 5 min. Pd(PPh₃)₄ (0.05 mmol) was then added, followed by purging and allowed the reaction mixture to stir at 90 °C for overnight. After completion of the reaction, product was extracted with ethyl acetate (2 × 50 ml). The combined organic layer was concentrated in vacuo

and crude reaction mixture was purified by silica gel (#100-200) column chromatography using EtOAc: hexane as eluent to get desired products **9a-x**.

4.6.1. *6-Phenyl-4-(4-cyanomethyl)phenylamino quinazoline (9a)*. Yield: 81%, brick red solid; m.p. 253-255 °C; HPLC purity: 96% ($t_R = 33.92$ min); ^1H NMR (DMSO- d_6 , 400 MHz): δ 10.01 (s, 1H), 8.85 (s, 1H), 8.60 (s, 1H), 8.21 (d, 1H, $J = 7.0$ Hz), 7.91-7.87 (m, 4H), 7.62-7.58 (m, 4H), 7.57-7.39 (m, 2H), 4.04 (s, 2H); ^{13}C NMR (DMSO- d_6 , 125 MHz): δ 157.83, 154.42, 149.01, 139.12, 138.49, 138.07, 131.79, 131.50, 131.42, 129.02, 128.78, 128.69, 128.37, 128.22, 127.92, 127.14, 126.39, 122.95, 120.45, 119.40, 115.33, 21.91; IR (CHCl₃): ν_{max} 3400, 2924, 2853, 1609, 1437, 1192, 1119 cm^{-1} ; HR-ESIMS: m/z 337.1452 calcd for C₂₂H₁₆N₄+H⁺ (337.1448).

4.6.2. *6-(2,4-Difluorophenyl)-4-(4-cyanomethyl)phenylamino quinazoline (9b)*. Yield: 45%; yellow solid; m.p. 186-188 °C; HPLC purity: 98% ($t_R = 30.25$ min); ^1H NMR (CDCl₃, 400 MHz): δ 8.74 (s, 1H), 8.15 (s, 1H), 7.98-7.92 (m, 2H), 7.80 (d, 1H, $J = 8.8$ Hz), 7.55-7.46 (m, 2H), 7.38 (d, 2H, $J = 8.4$ Hz), 7.06-6.97 (m, 2H), 3.78 (s, 2H); ^{19}F NMR (DMSO- d_6 , 376 MHz): δ -110.14 to -110.23 (m, 1F), -113.34 to -113.41 (m, 1F); ^{13}C NMR (CDCl₃ + CD₃OD, 100 MHz): δ 162.53 (d, $^1J_{CF} = 237$ Hz), 159.62 (d, $^1J_{CF} = 238$ Hz), 154.55, 148.49, 138.13, 133.96, 133.44, 131.60-131.46 (m), 128.23, 127.45, 125.79, 123.14, 121.90, 117.86, 115.31, 111.79-111.54 (m), 104.26 (t, $^2J_{CF} = 26$ Hz), 22.72; IR (CHCl₃): ν_{max} 3391, 2955, 2923, 2854, 1606, 1574, 1532, 1515, 1495, 1424, 1401, 1269, 1142, 1101, 1020 cm^{-1} ; HR-ESIMS: m/z 373.1258 calcd for C₂₂H₁₄F₂N₄+H⁺ (373.1259).

4.6.3. *6-(2-Formylphenyl)-4-(4-cyanomethyl)phenylamino quinazoline (9c)*. Yield: 67%; brick red solid; m.p. 177-179 °C; HPLC purity: 93% ($t_R = 28.7$ min); ^1H NMR (CDCl₃ + CD₃OD, 400 MHz): δ 9.99 (s, 1H), 8.80 (s, 1H), 8.32 (s, 1H), 8.12 (d, 1H, $J = 1.6$ Hz), 7.99 (t, 2H, $J = 8.8$ Hz), 7.84-7.76 (m, 2H), 7.71-7.62 (m, 1H), 7.57-7.48 (m, 2H), 7.43-7.39 (m, 1H), 7.32-7.30 (m,

1H), 3.74 (s, 2H); ¹³C NMR (CDCl₃ + CD₃OD, 100 MHz): δ 192.32, 154.88, 148.58, 144.54, 136.48, 134.82, 134.00, 133.56, 131.95, 131.85, 131.14, 128.73, 128.60, 128.45, 128.42, 128.22, 127.45, 123.72, 123.41, 118.03, 115.22, 22.88; IR (CHCl₃): ν_{max} 3369, 2956, 2924, 2854, 2250, 1689, 1626, 1596, 1571, 1529, 1515, 1479, 1423, 1402, 1360, 1307, 1252, 1194, 1173, 1120, 1070, 1021 cm⁻¹; HR-ESIMS: *m/z* 365.1397 calcd for C₂₃H₁₆N₄O+H⁺ (365.1397).

4.6.4. 6-(4-Acetylphenyl)-4-(4-cyanomethyl)phenylamino quinazoline (**9d**). Yield: 45%; pale yellow solid; m.p. 157-159 °C; HPLC purity: 93% (*t_R* = 31.16 min); ¹H NMR (CDCl₃ + CD₃OD, 400 MHz): δ 8.65 (d, 1H, *J* = 9.0 Hz), 8.12 (t, 2H, *J* = 8.5 Hz), 7.95-7.91 (m, 2H), 7.83-7.82 (m, 1H), 7.42 (s, 2H), 7.41 (s, 1H), 7.40 (s, 3H), 3.84 (s, 2H), 2.70 (s, 3H); ¹³C NMR (DMSO-*d*₆, 125 MHz): δ 197.59, 157.93, 154.87, 149.53, 143.38, 138.36, 136.63, 135.90, 132.05, 131.50, 131.42, 128.95, 128.80, 128.71, 128.58, 128.26, 127.27, 126.57, 123.08, 121.20, 119.41, 115.33, 26.85, 21.90; IR (CHCl₃): ν_{max} 3369, 2953, 2924, 2855, 2250, 1738, 1678, 1603, 1573, 1532, 1515, 1424, 1362, 1265, 1020 cm⁻¹; HR-ESIMS: *m/z* 379.1555 calcd for C₂₄H₁₈N₄O+H⁺ (379.1553).

4.6.5. 6-(3-Hydroxyphenyl)-4-(4-cyanomethyl)phenylamino quinazoline (**9e**). Yield: 62%; brown solid; m.p. 222-224 °C; HPLC purity: 98% (*t_R* = 32.75 min); ¹H NMR (DMSO-*d*₆, 400 MHz): δ 10.01 (s, 1H), 9.65 (s, 1H), 8.81 (d, 1H, *J* = 1.6 Hz), 8.59 (s, 1H), 8.13 (dd, 1H, *J* = 8.4, 2.0 Hz), 7.90-7.84 (m, 2H), 7.65-7.55 (m, 4H), 7.41-7.26 (m, 2H), 6.87-6.85 (m, 1H), 4.05 (s, 2H); ¹³C NMR (DMSO-*d*₆, 100 MHz): δ 157.89, 157.85, 154.34, 149.01, 140.59, 138.53, 138.28, 131.76, 129.99, 128.29, 128.19, 126.36, 122.96, 120.33, 119.35, 117.95, 115.30, 114.87, 114.05, 21.91; IR (CHCl₃): ν_{max} 3400, 3055, 2955, 2924, 2854, 1731, 1591, 1484, 1437, 1400, 1275, 1219, 1189, 1119, 1072, 1020 cm⁻¹; HR-ESIMS: *m/z* 353.1402 calcd for C₂₂H₁₆N₄O+H⁺ (353.1397).

4.6.6. 6-(3-Nitrophenyl)-4-(4-cyanomethyl)phenylamino quinazoline (**9f**). Yield: 57%; pale yellow solid; m.p. 216-218 °C; HPLC purity: 95% ($t_R = 33.91$ min); ^1H NMR (CDCl₃ + CD₃OD, 400 MHz): δ 8.69 (d, 2H, $J = 8.4$ Hz), 8.29 (d, 1H, $J = 8.0$ Hz), 8.14 (d, 1H, $J = 7.2$ Hz), 7.97 (d, 1H, $J = 8.8$ Hz), 7.83 (d, 2H, $J = 8.0$ Hz), 7.73 (t, 1H, $J = 8.0$ Hz), 7.65-7.58 (m, 2H), 7.51 (s, 2H), 3.84 (s, 2H); ^{13}C NMR (CDCl₃ + CD₃OD, 125 MHz): δ 158.67, 154.75, 148.69, 141.30, 136.79, 133.06, 132.30, 131.87, 131.77, 131.69, 129.94, 128.59, 128.49, 128.29, 127.99, 126.09, 123.36, 122.37, 121.85, 120.86, 117.96, 22.63; IR (CHCl₃): ν_{max} 3401, 2955, 2923, 2853, 1733, 1607, 1536, 1423, 1384, 1157, 1021 cm⁻¹; HR-ESIMS: m/z 382.1302 calcd for C₂₂H₁₅N₅O₂+H⁺ (382.1299).

4.6.7. 6-(2-Methylphenyl)-4-(4-cyanomethyl)phenylamino quinazoline (**9g**). Yield: 57%; orange solid; m.p. 173-175 °C; HPLC purity: 95% ($t_R = 33.79$ min); ^1H NMR (CDCl₃, 400 MHz): δ 8.83-8.81 (m, 1H), 8.03-8.00 (m, 1H), 7.98-7.96 (m, 4H), 7.55 (s, 1H), 7.43-7.27 (m, 6H), 3.78 (s, 2H), 2.32 (s, 3H); ^{13}C NMR (CDCl₃, 100 MHz): δ 157.67, 154.73, 148.95, 140.83, 140.54, 138.33, 135.42, 134.63, 130.60, 129.79, 128.64, 128.37, 128.09, 126.06, 125.66, 122.52, 120.74, 117.97, 115.07, 23.14, 20.47; IR (CHCl₃): ν_{max} 3368, 2955, 2924, 2853, 2252, 1626, 1604, 1572, 1527, 1515, 1486, 1421, 1403, 1360, 1307, 1242, 1190, 1020 cm⁻¹; HR-ESIMS: m/z 351.1602 calcd for C₂₃H₁₈N₄+H⁺ (351.1604).

4.6.8. 6-(4-Vinylphenyl)-4-(4-cyanomethyl)phenylamino quinazoline (**9h**). Yield: 71%; pale yellow solid; m.p. 216-218 °C; HPLC purity: 93% ($t_R = 35.16$ min); ^1H NMR (CDCl₃ + CD₃OD, 400 MHz): δ 8.58 (d, 1H, $J = 17.2$ Hz), 8.10 (d, 1H, $J = 8.4$ Hz), 7.89 (d, 1H, $J = 8.4$ Hz), 7.82-7.75 (m, 4H), 7.60-7.51 (m, 3H), 7.44-7.39 (m, 2H), 6.83-6.76 (m, 1H), 5.85 (d, 1H, $J = 17.6$ Hz), 5.33 (d, 1H, $J = 10.8$ Hz), 3.84 (s, 2H); ^{13}C NMR (DMSO-*d*₆, 125 MHz): δ 158.30, 154.92, 149.57, 138.96, 138.87, 137.93, 137.19, 136.56, 132.05, 131.97, 128.89, 128.70, 127.72, 127.27,

126.90, 123.48, 120.64, 119.87, 115.83, 115.30, 22.39; IR (CHCl₃): ν_{\max} 3369, 2951, 2923, 2857, 2248, 1741, 1623, 1603, 1571, 1514, 1497, 1423, 1360, 1021 cm⁻¹; HR-ESIMS: m/z 363.1605 calcd for C₂₄H₁₈N₄+H⁺ (363.1604).

4.6.9. *6-(4-Fluorobenzyloxyphen-4-yl)-4-(4-cyanomethyl)phenylamino quinazoline (9i)*. Yield: 58%; pale yellow solid; m.p. 230-232 °C; HPLC purity: 96% (t_R = 33.92 min); ¹H NMR (CDCl₃ + CD₃OD, 500 MHz): δ 8.61 (s, 1H), 8.45 (s, 1H), 8.04 (d, 1H, J = 2.0 Hz), 7.88 (d, 1H, J = 8.8 Hz), 7.81 (d, 2H, J = 8.4 Hz), 7.73-7.70 (m, 2H), 7.47 (d, 2H, J = 5.4 Hz), 7.45-7.39 (m, 3H), 7.13-7.11 (m, 3H), 5.12 (s, 2H), 3.83 (s, 2H); ¹³C NMR (CDCl₃ + CD₃OD, 125 MHz): δ 158.42, 153.75, 147.84, 139.15, 132.26 (d, ² J_{CF} = 37.5 Hz), 129.20, 129.13, 128.17, 127.26, 125.84, 123.26, 119.11, 117.95, 115.59, 115.21, 115.08, 115.04, 69.15, 22.50; ¹⁹F NMR (DMSO-*d*₆, 376 MHz): δ -114.38 to -114.45 (m, 1F); IR (CHCl₃): ν_{\max} 3400, 2955, 2923, 2854, 1605, 1573, 1498, 1514, 1423, 1401, 1384, 1225, 1157, 1020 cm⁻¹; HR-ESIMS: m/z 461.1777 calcd for C₂₉H₂₁FN₄O+H⁺ (461.1772).

4.6.10. *6-(3-Acetylaminophenyl)-4-(4-cyanomethyl)phenylamino quinazoline (9j)*. Yield: 61%; pale yellow solid; m.p. 195-197 °C; HPLC purity: 92% (t_R = 34.26 min); ¹H NMR (DMSO-*d*₆, 400 MHz): δ 10.10 (s, 1H), 10.01 (s, 1H), 8.80 (d, 1H, J = 1.2 Hz), 8.60 (s, 1H), 8.09 (dd, 1H, J = 8.8, 1.6 Hz), 8.00 (s, 1H), 7.89 (dd, 3H, J = 8.8, 1.6 Hz), 7.66-7.46 (m, 3H), 7.39 (d, 2H, J = 8.4 Hz), 4.04 (s, 2H), 2.09 (s, 3H); ¹³C NMR (DMSO-*d*₆, 125 MHz): δ 168.40, 157.79, 154.38, 148.98, 139.85, 139.80, 138.43, 138.23, 131.42, 131.34, 129.30, 128.71, 128.61, 128.38, 128.14, 126.32, 122.87, 122.05, 120.57, 119.31, 118.50, 117.79, 115.26, 23.95, 21.83; IR (CHCl₃): ν_{\max} 3368, 2921, 1676, 1608, 1534, 1515, 1480, 1426, 1119 cm⁻¹; HR-ESIMS: m/z 394.1667 calcd for C₂₄H₁₉N₅O+H⁺ (394.1662).

4.6.11. 6-(4-Phenylphenyl)-4-(4-cyanomethyl)phenylamino quinazoline (**9k**). Yield: 54%; yellow solid; m.p. 214-216 °C; HPLC purity: 99% ($t_R = 34.25$ min); ^1H NMR (DMSO- d_6 , 400 MHz): δ 10.03 (s, 1H), 8.92 (d, 1H, $J = 1.6$ Hz), 8.61 (s, 1H), 8.29-8.27 (m, 1H), 8.03 (d, 2H, $J = 8.4$ Hz), 7.92-7.87 (m, 5H), 7.80 (d, 2H, $J = 1.2$ Hz), 7.52 (t, 2H, $J = 7.6$ Hz), 7.43-7.40 (m, 3H), 4.01 (s, 2H); ^{13}C NMR (DMSO- d_6 , 125 MHz): δ 157.84, 154.47, 149.11, 139.59, 139.41, 138.46, 138.01, 137.44, 131.64, 129.02, 128.47, 128.25, 127.69, 127.62, 127.25, 126.65, 123.03, 120.27, 119.42, 115.38, 21.90; IR (CHCl₃): ν_{max} 3401, 2953, 2927, 1604, 1567, 1515, 1486, 1423, 1358, 1021 cm⁻¹; HR-ESIMS: m/z 413.1769 calcd for C₂₈H₂₀N₄+H⁺ (413.1761).

4.6.12. 6-(4-(4-Ethoxyphenyl)phenyl)-4-(4-cyanomethyl)phenylamino quinazoline (**9l**). Yield: 47%; brown solid; m.p. 195-197 °C; HPLC purity: 99% ($t_R = 37.33$ min); ^1H NMR (DMSO- d_6 , 400 MHz): δ 10.04 (s, 1H), 8.91 (s, 1H), 8.61 (s, 1H), 8.27 (d, 1H, $J = 8.8$ Hz), 7.99 (d, 2H, $J = 8.8$ Hz), 7.91-7.88 (m, 3H), 7.83 (d, 2H, $J = 8.4$ Hz), 7.72 (d, 2H, $J = 8.4$ Hz), 7.41 (d, 2H, $J = 8.4$ Hz), 7.06 (d, 2H, $J = 8.8$ Hz), 4.12-4.07 (m, 2H), 4.06 (s, 2H), 1.37 (t, 3H, $J = 6.8$ Hz); ^{13}C NMR (DMSO- d_6 , 125 MHz): δ 158.37, 157.85, 154.41, 149.03, 139.31, 138.48, 137.56, 137.22, 131.58, 128.43, 128.24, 127.73, 127.54, 126.63, 123.02, 120.08, 114.90, 63.12, 21.91, 14.64; IR (CHCl₃): ν_{max} 3306, 2956, 2925, 2855, 1729, 1604, 1568, 1515, 1494, 1424, 1401, 1360, 1252, 1190, 1082, 1019 cm⁻¹; HR-ESIMS: m/z 457.2012 calcd for C₃₀H₂₄N₄O+H⁺ (457.2023).

4.6.13. 6-(4-Phenyl-2-fluorophenyl)-4-(4-cyanomethyl)phenylamino quinazoline (**9m**). Yield: 57%; pale yellow solid; m.p. 229-231 °C; HPLC purity: 98% ($t_R = 34.64$ min); ^1H NMR (CDCl₃ + CD₃OD, 400 MHz): δ 8.64-8.61 (m, 2H), 8.13 (dd, 1H, $J = 8.4, 2.0$ Hz), 7.93 (d, 1H, $J = 8.8$ Hz), 7.83 (d, 2H, $J = 8.4$ Hz), 7.68-7.61 (m, 4H), 7.51-7.47 (m, 2H), 7.43-7.38 (m, 4H), 3.85 (s, 2H); ^{19}F NMR (DMSO- d_6 , 376 MHz): δ -117.72 (t, 1F, $J = 11.3$ Hz); ^{13}C NMR (CDCl₃ + CD₃OD, 125 MHz): δ 162.53, 160.56, 160.21, 155.89, 150.11, 142.10, 139.31, 136.60, 133.53,

132.63, 132.60, 130.25, 130.22, 129.86, 129.83, 129.23, 129.15, 127.63, 124.94, 124.43, 121.75, 119.58, 117.2, 116.07 (d, $^2J_{CF} = 23.7$ Hz), 24.13; IR (CHCl₃): ν_{\max} 3392, 2951, 2924, 2853, 2250, 1604, 1573, 1515, 1483, 1424, 1021 cm⁻¹; HR-ESIMS: m/z 431.1666 calcd for C₂₈H₁₉FN₄+H⁺ (431.1667).

4.6.14. 6-(Naphthalen-2-yl)-4-(4-cyanomethyl)phenylamino quinazoline (**9n**). Yield: 57%; pale yellow solid; m.p. 204-206 °C; HPLC purity: 91% ($t_R = 36.18$ min); ¹H NMR (DMSO-*d*₆, 400 MHz): δ 9.98 (s, 1H), 8.93 (d, 1H, $J = 1.6$ Hz), 8.55 (s, 1H), 8.37 (s, 1H), 8.30 (dd, 1H, $J = 8.8, 2.0$ Hz), 8.04 (s, 2H), 7.98 (d, 1H, $J = 7.2$ Hz), 7.93 (d, 1H, $J = 6.8$ Hz), 7.87-7.83 (m, 2H), 7.54-7.50 (m, 3H), 7.34 (d, 2H, $J = 8.4$ Hz), 3.98 (s, 2H); ¹³C NMR (DMSO-*d*₆, 125 MHz): δ 157.85, 154.48, 149.12, 136.42, 133.24, 132.34, 132.00, 131.46, 131.38, 128.75, 128.66, 128.56, 128.46, 128.20, 127.55, 126.59, 126.42, 126.39, 125.78, 125.28, 123.03, 120.69, 115.40, 21.89; IR (CHCl₃): ν_{\max} 3369, 3053, 2955, 2924, 2854, 2250, 1733, 1603, 1572, 1529, 1515, 1468, 1422, 1404, 1385, 1361, 1245, 1175, 1119, 1070, 1020 cm⁻¹; HR-ESIMS: m/z 387.1611 calcd for C₂₆H₁₈N₄+H⁺ (387.1604).

4.6.15. 6-(2,3-Dihydrobenzo[*b*][1,4]dioxin-6-yl)-4-(4-cyanomethyl)phenylamino quinazoline (**9o**). Yield: 69%; pale yellow solid; m.p. 207-209 °C; HPLC purity: 96% ($t_R = 30.66$ min); ¹H NMR (DMSO-*d*₆, 400 MHz): δ 9.95 (s, 1H), 8.76 (d, 1H, $J = 1.6$ Hz), 8.57 (s, 1H), 8.15 (dd, 1H, $J = 8.8, 2.0$ Hz), 7.89 (d, 2H, $J = 8.4$ Hz), 7.82 (d, 1H, $J = 8.8$ Hz), 7.65-7.53 (m, 1H), 7.46 (d, 1H, $J = 2.0$ Hz), 7.41-7.37 (m, 2H), 7.03 (d, 1H, $J = 8.4$ Hz), 4.32 (s, 4H), 4.05 (s, 2H); ¹³C NMR (CDCl₃ + CD₃OD, 125 MHz): δ 158.43, 153.87, 148.00, 143.73, 143.59, 139.00, 133.02, 132.12, 131.78, 131.70, 128.59, 128.49, 128.24, 127.37, 125.78, 123.26, 120.13, 119.17, 118.00, 117.58, 115.79, 64.32, 64.26, 22.65; IR (CHCl₃): ν_{\max} 3400, 2922, 2853, 1602, 1514, 1495, 1422, 1307, 1249, 1068, 1021 cm⁻¹; HR-ESIMS: m/z 395.1508 calcd for C₂₄H₁₈N₄O₂+H⁺ (395.1503).

4.6.16. 6-(Benzo[d][1,3]dioxol-5-yl)-4-(4-cyanomethyl)phenylamino quinazoline (**9p**). Yield: 57%; yellow solid; m.p. 241-243 °C; HPLC purity: 91% ($t_R = 29.68$ min); ^1H NMR (DMSO- d_6 , 400 MHz): δ 9.90 (s, 1H), 8.76 (d, 1H, $J = 1.6$ Hz), 8.58 (s, 1H), 8.23-8.15 (m, 1H), 7.99-7.81 (m, 3H), 7.53 (d, 1H, $J = 1.6$ Hz), 7.41-7.39 (m, 2H), 7.12 (d, 1H, $J = 4.8$ Hz), 6.12 (s, 2H), 4.05 (s, 2H); ^{13}C NMR (DMSO- d_6 , 100 MHz): δ 157.74, 154.21, 148.78, 148.13, 147.26, 138.52, 137.73, 133.28, 131.58, 128.25, 128.20, 126.38, 122.95, 120.85, 119.71, 119.33, 115.29, 108.74, 107.42, 101.32, 21.91; IR (CHCl₃): ν_{max} 3400, 2923, 1603, 1514, 1419, 1220, 1039 cm⁻¹; HR-ESIMS: m/z 381.1317 calcd for C₂₃H₁₆N₄O₂+H⁺ (381.1346).

4.6.17. 6-(Benzofuran-2-yl)-4-(4-cyanomethyl)phenylamino quinazoline (**9q**). Yield: 62%; pale yellow solid; m.p. 245-247 °C; HPLC purity: 92% ($t_R = 32.17$ min); ^1H NMR (DMSO- d_6 , 400 MHz): δ 10.14 (s, 1H), 9.09 (d, 1H, $J = 1.6$ Hz), 8.61 (s, 1H), 8.41-8.38 (m, 1H), 7.93-7.88 (m, 2H), 7.75 (d, 1H, $J = 7.2$ Hz), 7.71-7.69 (m, 1H), 7.65-7.60 (m, 2H), 7.58-7.53 (m, 1H), 7.42-7.39 (m, 2H), 7.32-7.30 (m, 1H), 4.06 (s, 2H); ^{13}C NMR (DMSO- d_6 , 125 MHz): δ 157.84, 154.88, 154.57, 154.46, 149.84, 138.42, 131.50, 131.42, 128.79, 128.70, 128.65, 128.23, 125.09, 123.46, 123.06, 121.45, 119.42, 118.65, 115.39, 111.15, 103.34, 21.91; IR (CHCl₃): ν_{max} 3400, 2955, 2923, 2853, 1605, 1572, 1515, 1422, 1385, 1020 cm⁻¹; HR-ESIMS: m/z 377.1399 calcd for C₂₄H₁₆N₄O+H⁺ (377.1397).

4.6.18. 6-(Benzo[b]thiophen-2-yl)-4-(4-cyanomethyl)phenylamino quinazoline (**9r**). Yield: 65%; yellow solid; m.p. 263-265 °C; HPLC purity: 98% ($t_R = 32.98$ min); ^1H NMR (DMSO- d_6 , 400 MHz): δ 10.04 (s, 1H), 8.91 (s, 1H), 8.58 (s, 1H), 8.24 (dd, 1H, $J = 8.4, 2.0$ Hz), 8.05-8.02 (m, 2H), 7.91-7.84 (m, 4H), 7.44-7.38 (m, 4H), 4.02 (s, 2H); ^{13}C NMR (DMSO- d_6 , 100 MHz): δ 157.69, 154.65, 149.52, 142.35, 140.22, 138.89, 138.30, 131.42, 130.88, 128.63, 128.14, 126.51, 124.90, 124.86, 123.76, 123.09, 122.45, 121.09, 119.89, 119.25, 115.36, 21.85; IR (CHCl₃): ν_{max}

3392, 2951, 2922, 2852, 1603, 1572, 1514, 1419, 1403, 1361, 1157, 1020 cm^{-1} ; HR-ESIMS: m/z 393.1163 calcd for $\text{C}_{24}\text{H}_{16}\text{N}_4\text{S}+\text{H}^+$ (393.1168).

4.6.19. 6-(Dibenzo(*b,d*)furan-4-yl)-4-(4-cyanomethyl)phenylamino quinazoline (**9s**). Yield: 42%; pale yellow solid; m.p. 207-209 °C; HPLC purity: 93% (t_R = 37.87 min); ^1H NMR (DMSO- d_6 , 400 MHz): δ 10.03 (s, 1H), 9.02 (d, 1H, J = 1.6 Hz), 8.66 (s, 1H), 8.46 (dd, 1H, J = 8.8, 2.0 Hz), 8.26-8.23 (m, 2H), 7.99 (d, 1H, J = 8.8 Hz), 7.91 (d, 3H, J = 8.0 Hz), 7.79 (d, 1H, J = 8.0 Hz), 7.65-7.55 (m, 3H), 7.48-7.39 (m, 2H), 4.05 (s, 2H); ^{13}C NMR ($\text{CDCl}_3 + \text{CD}_3\text{OD}$, 125 MHz): δ 156.04, 154.55, 153.18, 148.63, 134.29, 131.94, 131.86, 128.70, 128.60, 128.44, 127.50, 127.02, 123.39, 123.31, 123.04, 120.76, 120.44, 111.73, 22.93; IR (CHCl_3): ν_{max} 3392, 2955, 2923, 2853, 1604, 1573, 1530, 1515, 1490, 1451, 1402, 1362, 1189, 1120, 1020 cm^{-1} ; HR-ESIMS: m/z 427.1553 calcd for $\text{C}_{28}\text{H}_{18}\text{N}_4\text{O}+\text{H}^+$ (427.1553).

4.6.20. 6-(Dibenzo(*b,d*)thiophene-4-yl)-4-(4-cyanomethyl)phenylamino quinazoline (**9t**). Yield: 45%; pale yellow solid; m.p. 199-201 °C; HPLC purity: 91% (t_R = 34.88 min); ^1H NMR ($\text{CDCl}_3 + \text{CD}_3\text{OD}$, 400 MHz): δ 8.57 (s, 1H), 8.17-8.15 (m, 2H), 7.89 (d, 1H, J = 8.8 Hz), 7.78-7.70 (m, 2H), 7.56-7.51 (m, 5H), 7.44-7.39 (m, 3H), 7.30 (d, 1H, J = 8.8 Hz), 3.75 (s, 2H); ^{13}C NMR ($\text{CDCl}_3 + \text{CD}_3\text{OD}$, 125 MHz): δ 148.58, 139.38, 138.51, 135.59, 133.53, 132.46, 132.43, 131.94, 131.86, 128.75, 128.66, 128.42, 127.22, 127.04, 126.17, 125.26, 124.61, 123.53, 122.59, 122.01, 121.80, 121.07, 118.12, 22.79; IR (CHCl_3): ν_{max} 3392, 2922, 2853, 1605, 1571, 1537, 1514, 1421, 1026 cm^{-1} ; HR-ESIMS: m/z 443.1320 calcd for $\text{C}_{28}\text{H}_{18}\text{N}_4\text{S}+\text{H}^+$ (443.1325).

4.6.21. 6-(1*H*-Indol-5-yl)-4-(4-cyanomethyl)phenylamino quinazoline (**9u**). Yield: 63%; brown solid; m.p. 267-269 °C; HPLC purity: 95% (t_R = 29.14 min); ^1H NMR (DMSO- d_6 , 400 MHz): δ 11.23 (s, 1H), 9.99 (s, 1H), 8.85 (d, 1H, J = 1.2 Hz), 8.58 (s, 1H), 8.23 (dd, 1H, J = 8.8, 1.6 Hz), 8.08 (s, 1H), 7.93-7.84 (m, 3H), 7.66-7.53 (m, 3H), 7.44-7.39 (m, 2H), 6.55 (s, 1H),

4.05 (s, 2H); ^{13}C NMR (DMSO- d_6 , 125 MHz): δ 157.70, 153.86, 148.37, 139.94, 138.63, 135.70, 131.50, 131.42, 130.21, 128.79, 128.70, 128.27, 128.19, 126.39, 126.25, 122.94, 120.72, 119.57, 119.43, 118.79, 111.91, 101.61, 21.90; IR (CHCl₃): ν_{max} 3212, 2923, 2853, 1603, 1572, 1529, 1514, 1437, 1421, 1309, 1175, 1119, 1070 cm^{-1} ; HR-ESIMS: m/z 376.1564 calcd for C₂₄H₁₇N₅+H⁺ (376.1557).

4.6.22. 6-(Quinolin-3-yl)-4-(4-cyanomethyl)phenylamino quinazoline (**9v**). Yield: 49%; off-white solid; m.p. 225-227 °C; HPLC purity: 99% (t_{R} = 31.57 min); ^1H NMR (DMSO- d_6 , 400 MHz): δ 10.06 (s, 1H), 9.52 (d, 1H, J = 2.0 Hz), 9.10 (d, 1H, J = 1.6 Hz), 8.86 (d, 1H, J = 2.0 Hz), 8.64 (s, 1H), 8.45-8.42 (m, 1H), 8.12 (d, 2H, J = 8.4 Hz), 7.97 (d, 3H, J = 8.4 Hz), 7.91 (d, 1H, J = 8.4 Hz), 7.83 (d, 1H, J = 1.2 Hz), 7.42 (d, 2H, J = 8.8 Hz), 4.05 (s, 2H); ^{13}C NMR (DMSO- d_6 , 125 MHz): δ 157.87, 154.84, 149.70, 149.42, 146.93, 138.39, 134.89, 133.29, 131.95, 131.82, 129.86, 128.74, 128.45, 128.27, 127.58, 127.27, 126.55, 123.01, 121.18, 119.38, 115.44, 21.92; IR (CHCl₃): ν_{max} 3400, 2922, 1617, 1423, 1130 cm^{-1} ; HR-ESIMS: m/z 388.1559 calcd for C₂₅H₁₇N₅+H⁺ (388.1557).

4.6.23. 6-(Pyridin-4-yl)-4-(4-cyanomethyl)phenylamino quinazoline (**9w**). Yield: 61%; pale yellow solid; m.p. 234-236 °C; HPLC purity: 99% (t_{R} = 25.18 min); ^1H NMR (CDCl₃ + CD₃OD, 400 MHz): δ 8.69-8.62 (m, 3H), 8.09 (t, 1H, J = 1.6 Hz), 7.97 (d, 1H, J = 8.4 Hz), 7.83 (d, 4H, J = 8.4 Hz), 7.41-7.32 (m, 3H), 3.81 (s, 2H). ^{13}C NMR (CDCl₃ + CD₃OD, 125 MHz): δ 158.51, 154.91, 149.30, 147.56, 137.93, 135.52, 131.31, 128.13, 127.95, 125.94, 123.18, 121.70, 120.98, 117.80, 115.54, 22.50; IR (CHCl₃): ν_{max} 3392, 2957, 2923, 2850, 1606, 1573, 1532, 1493, 1425, 1021 cm^{-1} ; HR-ESIMS: m/z 338.1365 calcd for C₂₁H₁₅N₅+H⁺ (338.1400).

4.6.24. 6-(Isoquinolin-4-yl)-4-(4-cyanomethyl)phenylamino quinazoline (**9x**). Yield: 37%; pale yellow solid; m.p. 237-239 °C; HPLC purity: >99% (t_{R} = 32.66 min); ^1H NMR (DMSO- d_6 ,

400 MHz): δ 9.90 (s, 1H), 9.45 (s, 1H), 8.81 (s, 1H), 8.69 (s, 1H), 8.63 (s, 1H), 8.30 (d, 1H, $J = 8.0$ Hz), 8.06 (dd, 1H, $J = 8.8, 1.6$ Hz), 7.98 (d, 1H, $J = 8.8$ Hz), 7.92-7.77 (m, 4H), 7.37 (d, 2H, $J = 8.8$ Hz), 4.03 (s, 2H); ^{13}C NMR (DMSO- d_6 , 125 MHz): δ 157.76, 154.84, 152.44, 149.23, 142.99, 138.46, 134.75, 134.55, 133.22, 131.71, 131.45, 128.20, 128.04, 127.97, 127.73, 126.36, 124.17, 124.10, 122.72, 119.35, 115.26, 21.89; IR (CHCl₃): ν_{max} 3400, 2923, 2853, 1624, 1423, 1042 cm⁻¹; HR-ESIMS: m/z 388.1564 calcd for C₂₅H₁₇N₅+H⁺ (388.1557).

4.7. PI3K- α assay. PI3K- α (diluted in 12.5 mM Glycine-NaOH (pH 8.5), 50 mM KCl, 2.5 mM MgCl₂, 1 mM DTT, 0.05% CHAPS) is assayed in total volume of 20 μL containing 12.5 mM glycine-NaOH (pH 8.5), 50 mM KCl, 2.5 mM MgCl₂, 1 mM DTT, 0.05% CHAPS, 0.01 mM ATP and 0.05 mM diC8 PIP2. The enzyme is assayed for 80 min after which 20 μL of ADP-Glo reagent is added. After a further incubation of 40 min, 40 μL of kinase detection buffer is added. The assays are incubated for 40 min and then read on PerkinElmer Envision for 1sec/well.

4.8. PI3K- β assay. PI3K beta (diluted in 12.5 mM glycine-NaOH (pH 8.5), 50 mM KCl, 2.5mM MgCl₂, 1 mM DTT, 0.05% CHAPS) is assayed in total volume of 20 μL containing 12.5 mM Glycine-NaOH (pH 8.5), 50 mM KCl, 2.5 mM MgCl₂, 1 mM DTT, 0.05% CHAPS, 0.01 mM ATP and 0.05 mM diC8 PIP2. The enzyme is assayed for 60 min after which 20 μL of ADP-Glo reagent is added. After a further incubation of 40 min, 40 μL of kinase detection buffer is added. The assays are incubated for 40 min and then read on PerkinElmer Envision for 1 sec/ well.

4.9. PI3K- δ assay. PI3K delta (diluted in 12.5 mM glycine-NaOH (pH 8.5), 50 mM KCl, 2.5 mM MgCl₂, 1 mM DTT, 0.05% CHAPS) is assayed in total volume of 20 μL containing 12.5 mM Glycine-NaOH (pH 8.5), 50 mM KCl, 2.5 mM MgCl₂, 1 mM DTT, 0.05% CHAPS, 0.01

mM ATP and 0.05 mM diC8 PIP2. The enzyme is assayed for 120 min after which 20 μ L of ADP-Glo reagent is added. After a further incubation of 40 min, 40 μ L of kinase detection buffer is added. The assays are incubated for 40 min and then read on PerkinElmer Envision for 1 sec/well.

4.10. PI3K- γ assay. PI3K gamma (diluted in 12.5 mM Glycine-NaOH (pH 8.5), 50 mM KCl, 2.5 mM MgCl₂, 1 mM DTT, 0.05% CHAPS) is assayed in total volume of 20 μ L containing 12.5 mM glycine-NaOH (pH 8.5), 50 mM KCl, 2.5 mM MgCl₂, 1 mM DTT, 0.05% CHAPS, 0.01 mM ATP and 0.05 mM diC8 PIP2. The enzyme is assayed for 75 min after which 20 μ L of ADP-Glo reagent is added. After a further incubation of 40 min, 40 μ L of kinase detection buffer is added. The assays are incubated for 40 min and then read on PerkinElmer Envision for 1sec/well. All PI3K assays were carried out at International center for kinase profiling, University of Dundee UK on commercial basis.

4.11. mTOR assay. mTOR assay was performed at Reaction Biology Corporation using the 'HotSpot' assay platform. Kinase assay protocol; reaction buffer: base reaction buffer; 20 mM Hepes (pH 7.5), 10 mM MgCl₂, 1 mM EGTA, 0.02% Brij35, 0.02 mg/ml BSA, 0.1 mM Na₃VO₄, 2 mM DTT, 1% DMSO. Required cofactors were added individually to kinase reaction. Reaction procedure: To a freshly prepared buffer solution was added required cofactor for the enzymatic reaction, followed by the addition of kinase at a concentration of 1 μ M. The contents were mixed gently, then the compounds under test dissolved in DMSO was added to the reaction mixture in the appropriate concentration. ³³P-ATP (specific activity 500 μ Ci/ μ L) was added to the mixture in order to initiate the reaction, and the mixture was incubated at room temperature for 2 h. All compounds were tested by single dose duplicate made at a concentration of 1 μ M. Reaction was

carried out at 10 μ M ATP concentration. Reaction was spotted onto P81 ion exchange paper and detected the kinase activity by filter-binding method.

4.12. In-vitro cytotoxicity. In-vitro cytotoxicity of all compounds was determined in five cancer cell lines *viz.* Panc-1 (pancreatic cancer), MCF-7 (breast cancer), PC-3 (prostate), HL-60 (leukemia) and A-375 (melanoma) using MTT assay. In each well of a 96-well plate, 3×10^3 cells were grown in 100 μ L of medium. After 24 h, each test molecules were added to achieve a final concentration of 10 to 0.01 μ mol/L, respectively. After 48 h of treatment, 20 μ L of 2.5 mg/mL MTT (Organics Research, Inc.) solution in phosphate buffer saline was added to each well. After 48h, supernatant was removed and formazan crystals were dissolved in 200 μ L of DMSO. Absorbance was then measured at 570 nm using an absorbance plate reader (Bio-Rad Microplate Reader). Data are expressed as the percentage of viable cells in treated relative to non-treated conditions. Each experiment was repeated thrice and data was expressed as mean \pm SD of three independent experiments [34].

4.13. Preparation of total cell lysates for immunoblotting. MCF-7 and PC-3 Cells (1×10^6) were collected, washed with cold PBS, and incubated with cold lysis buffer (50 mM Tris pH 8.0, 150 mM NaCl, 5 mM EDTA, 1% v/v Nonidet P-40, 1 mM PMSF, and 1% v/v eukaryotic protease inhibitor cocktail) for 30 min on ice. Cells were centrifuged at 12,000 g for 10 min at 4 $^{\circ}$ C, and the supernatant was collected as whole cell lysates for Western blot analysis of various proteins.

4.14. Western-blot analysis. The protein lysates prepared were subjected to discontinuous SDS-PAGE analysis. Proteins aliquots (50 μ g) were resolved on SDS-PAGE and then electro transferred to PVDF membrane overnight at 4 $^{\circ}$ C at 30 V. Nonspecific binding was blocked by incubation with 5% nonfat milk in tris-buffered saline containing 0.1% Tween-20 (TBST) for 1 h

at room temperature. The blots were probed with respective primary antibodies for 2 h and washed three times with TBST. The blots were then incubated with horseradish peroxidase conjugated mouse or rabbit secondary antibodies for 1 h, washed again three times with TBST, and signals detected using ECL plus Chemiluminescence's kit on X-ray film. Protein was measured employing the Bio-Rad protein assay kit using bovine serum albumin as the standard [35].

4.15. Cell cycle analysis by flow cytometry. The effect of compounds **9u** and **9x** on the DNA content was analysed by cell cycle phase distribution analysis in MCF-7 and PC-3 cells, respectively. Cells were incubated with **9u** and **9x** at indicated concentrations for 24 h time period. Cells were collected at 400 μ g, washed with ice-cold PBS and fixed with ice-cold 70% ethanol for overnight at 4 °C. Next day cells were incubated with RNase at concentration of 0.2 mg/mL at 37 °C for 1 h time period and stained with propidium iodide (10 μ g/mL) for 30 min in dark. Cells were analysed on flow-cytometer (FACS Calibur, Becton Dickinson) and data were collected in list mode on 10,000 events for FL2-A vs. FL2-W. Resulting DNA distributions were analyzed by Modfit (Verity Software House Inc., Topsham, ME) for the proportions of cells in apoptosis, G₁-phase, S- phase, and G₂-M phases of the cell cycle.

4.16. Flow cytometric determination of mitochondrial membrane potential. Change in mitochondrial transmembrane potential ($\Delta\Psi_m$) due to mitochondrial perturbation was measured after staining with Rhodamine-123. MCF-7 and PC-3 cells were incubated with the indicated doses of compounds **9u** and **9x**, respectively for 24 h. Rhodamine- 123 (5 μ M) was added 1 h before the termination of the experiment and cells were collected, washed in PBS. The fluorescence intensity of 10,000 events was analyzed in FL-1 channel on a BD FACS Calibur

(Becton Dickinson, USA) flow cytometer. The decrease in fluorescence intensity caused by loss of mitochondrial membrane potential was analyzed in FL-1 channel.

4.17. Determination of thermodynamic equilibrium solubility by 96-well plate-based assay. The compound was dissolved in methanol to get 2000 $\mu\text{g/mL}$ stock solution. The stock solution was introduced into 96-well plates and allowed to evaporate at room temperature to ensure that the compound (1, 2, 4, 8, 16, 25, 40, 80, 160 and 300 μg) is in solid form in the beginning of the experiment. Thereafter, 200 μl of the dissolution medium (water, PBS, SGF, and SIF) was added to the wells and plates were shaken horizontally at 300 rpm (Eppendorf Thermoblock Adapter, North America) for 4 h at room temperature (25 ± 1 $^{\circ}\text{C}$). The plates were covered with aluminium foil and were kept overnight for equilibration. Later, the plates were centrifuged at 3000 rpm for 15 min (Jouan centrifuge BR4i). Samples of 50 μl was withdrawn into UV 96-well plates (Corning® 96 Well Clear Flat Bottom UV-Transparent Microplate) for analyses with plate reader at corresponding λ_{max} of the sample (SpectraMax Plus384). The analysis was performed in triplicate for each compound. The solubility curve of concentration ($\mu\text{g/mL}$) vs absorbance was plotted to find out saturation point and the corresponding concentration was noted [36].

4.18. hrCYP P450 isoenzyme assay. hrCYP P450 isoenzyme were aliquoted as per the total concentration required to conduct the study and stored at -70 $^{\circ}\text{C}$ until use. Total assay volume was adjusted to 200 μL and consists of three components: cofactors, inhibitor/vehicle, and enzyme-substrate (ES) mix. The 50 μL of working cofactor stock solution was dispensed to all the specified wells in a black colored nunc microtiter polypropylene plate. The 50 μL of diluted working concentrations of test compounds/positive control/vehicle were dispensed in triplicate to the specified wells as per the plate map design. Reaction plate with cofactor and test item was

preincubated at 37 ± 1 °C in a shaking incubator for 10 min. Simultaneously, the ES mix was prepared by mixing the hrCYP P450 isoenzyme. Remaining volume was made up with the buffer and preincubated for 10 min at 37 ± 1 °C. Then 100 µL of ES mix was dispensed per well as per the plate map design and incubated at 37 ± 1 °C in shaking incubator for predetermined time. A set of controls were incubated with hrCYP P450 isoenzymes and substrate without test or reference item. A set of blanks were incubated with substrate and test or reference item, in the absence of hrCYP P450 isoenzymes. Reaction was terminated by adding specific quenching solutions (for CYP1A2, CYP2C19, and CYP3A4-75 µL of 100% acetonitrile, for CYP2C9-20 µL of 0.25 M Tris in 60% methanol, and for CYP2D6-75 µL of 0.25 M Tris in 60% methanol). The reaction was quenched by thoroughly mixing the final contents of the wells by repeated pipetting using multichannel pipet. The product fluorescence per well was measured using a multimode reader at excitation and emission wavelengths of respective hrCYP P450 isoenzyme fluorogenic metabolites. Data was analysed using Excel spreadsheet, and the % inhibition was calculated [37].

4.19. Caco-2 permeability assay. Permeability study was conducted with the Caco-2 monolayer cultured for 21 days (TEER full form values >500 cm² in each well) and by adding an appropriate volume of buffer (HBSS buffer containing 10 mM HEPES) containing test compounds to apical chamber. Test sample was taken from both apical and basolateral chambers at 0 and 90 min after incubation at 37 °C and analyzed by LC-MS/MS. Same experiment was repeated by adding an appropriate volume of buffer (HBSS buffer containing 10 mM HEPES) containing test compound to basolateral chamber. The AUC defined the net influx and outflow of the test compound across the Caco-2 cell monolayer.

4.20. *In vivo* anticancer activity of compounds 9u and 9x in Ehrlich Ascites Carcinoma (EAC) [38]. Ehrlich ascites carcinoma (EAC) cells were collected from the peritoneal cavity of the Swiss mice harbouring 8-10 days old ascitic tumor. 1×10^7 EAC cells were injected intraperitoneally in Swiss mice selected for the experiment on day 0. The next day, animals were randomized and divided into different groups. The treatment groups contained 7 animals each and control group contained 10 animals. Treatment groups were treated with 70 mg/kg of compound 9x and 25 mg/kg of compound 9u intraperitoneally from day 1-9. One more of the treatment groups received 5-fluorouracil (20 mg/kg, i.p) and it served as positive control. The tumor bearing control group was similarly administered normal saline (0.2 ml, i.p.). On day 12, animals were sacrificed and ascitic fluid was collected from peritoneal cavity of each mouse for the evaluation of tumor growth. Percent tumor growth inhibition was calculated based on the total number of tumor cells present in the peritoneal cavity as on day 12 of the experiment using the following formula.

$$\text{Percent tumor growth inhibition} = \frac{\text{Average no. of cells in control group} - \text{Average no. of cells in treated group}}{\text{Average no. of cells in treated group}} \times 100$$

4.21. *In vivo* anticancer activity of compound 9u in Ehrlich solid tumor model. Ehrlich ascites carcinoma (EAC) cells were collected from the peritoneal cavity of the swiss mice harbouring 8-10 days old ascitic tumor. 1×10^7 EAC cells were injected intramuscularly in right thigh of 31 swiss male mice selected for the experiment on day 0. The next day, animals were randomized and divided into four groups. Two treatment groups contained 7 animals each and one control group contained 10 animals. Treatment was given as follows:

Group I: 9u (15 mg/kg i/p) from day 1-9

Group II: **9u** (25 mg/kg i/p) from day 1-9

The third treatment group was treated with 5-fluorouracil (22 mg/kg, i.p) from day 1-9 and it served as positive control. The control group was similarly administered normal saline (0.2 ml, i.p.) from day 1-9. On day 9 and 13, tumor bearing thigh of each animal was shaved and longest and shortest diameters of the tumor were measured with the help of vernier caliper. Tumor weight of each animal was calculated using the following formula.

$$\text{Tumor weight (mg)} = \frac{\text{Length (mm)} \times [\text{width (mm)}]^2}{2}$$

The percent tumor growth inhibition was calculated on day 13 by comparing the average values of treated groups with that of control group. Tumor growth in saline treated control animals was taken to be 100%.

The experimental procedures employed in this study were approved by the Institutional Animal Ethics Committee, Indian Institute of Integrative Medicine, Jammu, India.

4.22. Molecular docking. The crystal structure of PI3K- α with co-crystallized ligand PI-103 (PDB: 4L23) [39] and PI3K- γ with pyrazolopyrimidine class of inhibitor (PDB: 3IBE) [40] were retrieved from protein data bank and were subjected to protein preparation wizard for filling missing loops and side chains (using Prime v3.1), H-bond optimization, heterogeneous state generation, protonation and overall minimization using OPLS-2005 force field. Grid file for docking was constructed considering PI-103 ligand as centroid of grid box of 10 Å size. All ligands were sketched in Maestro, prepared using ligprep and docked by induced fit docking

module using XP docking embedded in Maestro v9.3 defining flexible residues close enough of 10 Å distance to PI-103/pyrazolopyrimidine [30, 41].

ACKNOWLEDGEMENTS

RRY is thankful to CSIR, New Delhi for the award of senior research fellowship. V. K. is thankful to UGC for the award of research fellowship. P.J. is thankful to CSIR for senior research fellowship. S.S.B. is research associate (Reference No. 45/33/2013/NAN-BMS) receiving financial support from ICMR. The work was supported by CSIR 12th FYP grant # BSC-0205.

SUPPLEMENTARY DATA

Supporting information available. Experimental procedures and spectral data scans. This material is available free of charge via the internet at <http://sciencedirect.com>.

5. REFERENCES

- [1] J.A. Engelman, J. Luo, L.C. Cantley, The evolution of phosphatidylinositol 3-kinases as regulators of growth and metabolism, *Nat. Rev. Genet.*, 7 (2006) 606-619.
- [2] L.M. Thorpe, H. Yuzugullu, J.J. Zhao, PI3K in cancer: divergent roles of isoforms, modes of activation and therapeutic targeting, *Nat. Rev. Cancer*, 15 (2015) 7-24.
- [3] P. Liu, H. Cheng, T.M. Roberts, J.J. Zhao, Targeting the phosphoinositide 3-kinase pathway in cancer, *Nat. Rev. Drug Discov.*, 8 (2009) 627-644.
- [4] B. Vanhaesebroeck, J. Guillermet-Guibert, M. Graupera, B. Bilanges, The emerging mechanisms of isoform-specific PI3K signalling, *Nat. Rev. Mol. Cell Biol.*, 11 (2010) 329-341.

- [5] K. Okkenhaug, B. Vanhaesebroeck, PI3K in lymphocyte development, differentiation and activation, *Nat. Rev. Immunol.*, 3 (2003) 317-330.
- [6] J. Rodon, R. Dienstmann, V. Serra, J. Tabernero, Development of PI3K inhibitors: lessons learned from early clinical trials, *Nat. Rev. Clin. Oncol.*, 10 (2013) 143-153.
- [7] G. Powis, R. Bonjouklian, M.M. Berggren, A. Gallegos, R. Abraham, C. Ashendel, L. Zalkow, W.F. Matter, J. Dodge, G. Grindey, C.J. Vlahos, Wortmannin, a potent and selective inhibitor of phosphatidylinositol-3-kinase, *Cancer Res.*, 54 (1994) 2419-2423.
- [8] C.J. Vlahos, W.F. Matter, K.Y. Hui, R.F. Brown, A specific inhibitor of phosphatidylinositol 3-kinase, 2-(4-morpholinyl)-8-phenyl-4H-1-benzopyran-4-one (LY294002), *J. Biol. Chem.*, 269 (1994) 5241-5248.
- [9] L. Friedman, GDC-0941, a potent, selective, orally bioavailable inhibitor of class I PI3K, *Cancer Res.*, 68 (2008) LB-110.
- [10] M. Ehrhardt, R.B. Craveiro, M.I. Holst, T. Pietsch, D. Dilloo, The PI3K inhibitor GDC-0941 displays promising in vitro and in vivo efficacy for targeted medulloblastoma therapy, *Oncotarget*, 6 (2015) 802-813.
- [11] S.-M. Maira, F. Stauffer, J. Brueggen, P. Furet, C. Schnell, C. Fritsch, S. Brachmann, P. Chène, A. De Pover, K. Schoemaker, D. Fabbro, D. Gabriel, M. Simonen, L. Murphy, P. Finan, W. Sellers, C. García-Echeverría, Identification and characterization of NVP-BEZ235, a new orally available dual phosphatidylinositol 3-kinase/mammalian target of rapamycin inhibitor with potent in vivo antitumor activity, *Mol. Cancer Ther.*, 7 (2008) 1851-1863.

- [12] T.-J. Liu, D. Koul, T. LaFortune, N. Tiao, R.J. Shen, S.-M. Maira, C. Garcia-Echeverria, W.K.A. Yung, NVP-BEZ235, a novel dual phosphatidylinositol 3-kinase/mammalian target of rapamycin inhibitor, elicits multifaceted antitumor activities in human gliomas, *Mol. Cancer Ther.*, 8 (2009) 2204-2210.
- [13] S.-M. Maira, PI3K inhibitors for cancer treatment: Five years of preclinical and clinical research after BEZ235, *Mol. Cancer Ther.*, 10 (2011) 2016.
- [14] F.I. Raynaud, S.A. Eccles, S. Patel, S. Alix, G. Box, I. Chuckowree, A. Folkes, S. Gowan, A. De Haven Brandon, F. Di Stefano, A. Hayes, A.T. Henley, L. Lensun, G. Pergl-Wilson, A. Robson, N. Saghir, A. Zhyvoloup, E. McDonald, P. Sheldrake, S. Shuttleworth, M. Valenti, N.C. Wan, P.A. Clarke, P. Workman, Biological properties of potent inhibitors of class I phosphatidylinositide 3-kinases: from PI-103 through PI-540, PI-620 to the oral agent GDC-0941, *Mol. Cancer Ther.*, 8 (2009) 1725-1738.
- [15] D.A. Fruman, C. Rommel, PI3K and cancer: lessons, challenges and opportunities, *Nat. Rev. Drug Discov.*, 13 (2014) 140-156.
- [16] B.J. Lannutti, S.A. Meadows, S.E. Herman, A. Kashishian, B. Steiner, A.J. Johnson, J.C. Byrd, J.W. Tyner, M.M. Loriaux, M. Deininger, B.J. Druker, K.D. Puri, R.G. Ulrich, N.A. Giese, CAL-101, a p110delta selective phosphatidylinositol-3-kinase inhibitor for the treatment of B-cell malignancies, inhibits PI3K signaling and cellular viability, *Blood*, 117 (2011) 591-594.
- [17] P. Furet, V. Guagnano, R.A. Fairhurst, P. Imbach-Weese, I. Bruce, M. Knapp, C. Fritsch, F. Blasco, J. Blanz, R. Aichholz, J. Hamon, D. Fabbro, G. Caravatti, Discovery of NVP-

- BYL719 a potent and selective phosphatidylinositol-3 kinase alpha inhibitor selected for clinical evaluation, *Bioorg. Med. Chem. Lett.*, 23 (2013) 3741-3748.
- [18] C. Fritsch, A. Huang, C. Chatenay-Rivauday, C. Schnell, A. Reddy, M. Liu, A. Kauffmann, D. Guthy, D. Erdmann, A. De Pover, P. Furet, H. Gao, S. Ferretti, Y. Wang, J. Trappe, S.M. Brachmann, S.M. Maira, C. Wilson, M. Boehm, C. Garcia-Echeverria, P. Chene, M. Wiesmann, R. Cozens, J. Lehar, R. Schlegel, G. Caravatti, F. Hofmann, W.R. Sellers, Characterization of the novel and specific PI3Kalpha inhibitor NVP-BYL719 and development of the patient stratification strategy for clinical trials, *Mol. Cancer Ther.*, 13 (2014) 1117-1129.
- [19] Z.S. Zumsteg, N. Morse, G. Krigsfeld, G. Gupta, D.S. Higginson, N.Y. Lee, L. Morris, I. Ganly, S.L. Shiao, S.N. Powell, C.H. Chung, M. Scaltriti, J. Baselga, Taselisib (GDC-0032), a Potent β -Sparing Small Molecule Inhibitor of PI3K, Radiosensitizes Head and Neck Squamous Carcinomas Containing Activating PIK3CA Alterations, *Clin. Cancer Res.*, (2015) doi: 10.1158/1078-0432.CCR-1115-2245.
- [20] C.O. Ndubaku, T.P. Heffron, S.T. Staben, M. Baumgardner, N. Blaquiere, E. Bradley, R. Bull, S. Do, J. Dotson, D. Dudley, K.A. Edgar, L.S. Friedman, R. Goldsmith, R.A. Heald, A. Kolesnikov, L. Lee, C. Lewis, M. Nannini, J. Nonomiya, J. Pang, S. Price, W.W. Prior, L. Salphati, S. Sideris, J.J. Wallin, L. Wang, B. Wei, D. Sampath, A.G. Olivero, Discovery of 2-{3-[2-(1-isopropyl-3-methyl-1H-1,2,4-triazol-5-yl)-5,6-dihydrobenzo[f]imidazo[1,2-d][1,4]oxazepin-9-yl]-1H-pyrazol-1-yl}-2-methylpropanamide (GDC-0032): a β -sparing phosphoinositide 3-kinase inhibitor with high unbound exposure and robust in vivo antitumor activity, *J. Med. Chem.*, 56 (2013) 4597-4610.

- [21] K.A. Jessen, L. Kessler, J. Kucharski, X. Guo, J. Staunton, M. Elia, M. Janes, L. Lan, S. Wang, J. Stewart, L. Darjania, L. Li, K. Chan, M. Martin, P. Ren, D. Fruman, C. Rommel, Y. Liu, Abstract 4501: INK1117: A potent and orally efficacious PI3K α -selective inhibitor for the treatment of cancer, *Cancer Res.*, 71 (2011) 4501.
- [22] B. Barlaam, S. Cosulich, S. Degorce, M. Fitzek, S. Green, U. Hancox, C. Lambert-van der Brempt, J.J. Lohmann, M. Maudet, R. Morgentin, M.J. Pasquet, A. Peru, P. Ple, T. Saleh, M. Vautier, M. Walker, L. Ward, N. Warin, Discovery of (R)-8-(1-(3,5-difluorophenylamino)ethyl)-N,N-dimethyl-2-morpholino-4-oxo-4H-chromene-6-carboxamide (AZD8186): a potent and selective inhibitor of PI3K β and PI3K δ for the treatment of PTEN-deficient cancers, *J. Med. Chem.*, 58 (2015) 943-962.
- [23] O. Fjellstrom, D. Gustafsson, S. Jackson, J.A. Lindberg, Enantiomerically pure (-) 2-[1-(7-methyl-2-(morpholin-4-yl)-4-oxo-4h-pyrido[1,2-a]pyrimidin-9-yl)ethylamino]benzoic acid, its use in medical therapy, and a pharmaceutical composition comprising it - 026, WO/2009/093972, Astrazeneca AB (2009).
- [24] N. Liu, B.R. Rowley, C.O. Bull, C. Schneider, A. Haegebarth, C.A. Schatz, P.R. Fracasso, D.P. Wilkie, M. Hentemann, S.M. Wilhelm, W.J. Scott, D. Mumberg, K. Ziegelbauer, BAY 80-6946 is a highly selective intravenous PI3K inhibitor with potent p110 α and p110 δ activities in tumor cell lines and xenograft models, *Mol. Cancer Ther.*, 12 (2013) 2319-2330.
- [25] S.D. Knight, N.D. Adams, J.L. Burgess, A.M. Chaudhari, M.G. Darcy, C.A. Donatelli, J.I. Luengo, K.A. Newlander, C.A. Parrish, L.H. Ridgers, M.A. Sarpong, S.J. Schmidt, G.S. Van Aller, J.D. Carson, M.A. Diamond, P.A. Elkins, C.M. Gardiner, E. Garver, S.A. Gilbert, R.R. Gontarek, J.R. Jackson, K.L. Kershner, L. Luo, K. Raha, C.S. Sherk, C.-M.

- Sung, D. Sutton, P.J. Tummino, R.J. Wegrzyn, K.R. Auger, D. Dhanak, Discovery of gsk2126458, a highly potent inhibitor of pi3k and the mammalian target of rapamycin, *ACS Med. Chem. Lett.*, 1 (2010) 39-43.
- [26] H. Cheng, C. Li, S. Bailey, S.M. Baxi, L. Goulet, L. Guo, J. Hoffman, Y. Jiang, T.O. Johnson, T.W. Johnson, D.R. Knighton, J. Li, K.K.C. Liu, Z. Liu, M.A. Marx, M. Walls, P.A. Wells, M.-J. Yin, J. Zhu, M. Zientek, Discovery of the highly potent PI3K/mTOR dual inhibitor PF-04979064 through structure-based drug design, *ACS Med. Chem. Lett.*, 4 (2012) 91-97.
- [27] A.S. Wheeler, W.M. Oates, The bromination of anthranilic acid, *J. Am. Chem. Soc.*, 32 (1910) 770-773.
- [28] P. Johnström, A. Fredriksson, J.-O. Thorell, S. Stone-Elander, Synthesis of [methoxy-¹¹C]PD153035, a selective EGF receptor tyrosine kinase inhibitor, *J. Labelled Comp. Radiopharm.*, 41 (1998) 623-629.
- [29] A.J. Bridges, H. Zhou, D.R. Cody, G.W. Rewcastle, A. McMichael, H.D.H. Showalter, D.W. Fry, A.J. Kraker, W.A. Denny, Tyrosine kinase inhibitors. 8. An unusually steep structure-activity relationship for analogues of 4-(3-bromoanilino)-6,7-dimethoxyquinazoline (PD 153035), a potent inhibitor of the epidermal growth factor receptor, *J. Med. Chem.*, 39 (1996) 267-276.
- [30] D.A. Sabbah, J.L. Vennerstrom, H. Zhong, Docking studies on isoform-specific inhibition of phosphoinositide-3-kinases, *J. Chem. Inf. Model*, 50 (2010) 1887-1898.

- [31] D. King, D. Yeomanson, H.E. Bryant, PI3King the lock: targeting the PI3K/Akt/mTOR pathway as a novel therapeutic strategy in neuroblastoma, *J. Pediatr. Hematol. Oncol.*, 37 (2015) 245-251.
- [32] X. Li, C. Wu, N. Chen, H. Gu, A. Yen, L. Cao, E. Wang, L. Wang, PI3K/Akt/mTOR signaling pathway and targeted therapy for glioblastoma, *Oncotarget*, (2016) doi: 10.18632/oncotarget.17961.
- [33] J.J. Lee, K. Loh, Y.S. Yap, PI3K/Akt/mTOR inhibitors in breast cancer, *Cancer Biol. Med.*, 12 (2015) 342-354.
- [34] S. Bhushan, J. Singh, M.J. Rao, A.K. Saxena, G.N. Qazi, A novel lignan composition from *Cedrus deodara* induces apoptosis and early nitric oxide generation in human leukemia Molt -4 and HL-60 cells, *Nitric Oxide*, 14 (2006) 72-88.
- [35] S. Bhushan, A. Kumar, F. Malik, S. Andotra, V. Sethi, I. Kaur, S. Taneja, G. Qazi, J. Singh, A triterpenediol from *Boswellia serrata* induces apoptosis through both the intrinsic and extrinsic apoptotic pathways in human leukemia HL-60 cells, *Apoptosis*, 12 (2007) 1911-1926.
- [36] S.S. Bharate, R.A. Vishwakarma, Thermodynamic equilibrium solubility measurements in simulated fluids by 96-well plate method in early drug discovery, *Bioorg. Med. Chem. Lett.*, 25 (2015) 1561-1567.
- [37] C.L. Crespi, V.P. Miller, B.W. Penman, Microtiter plate assays for inhibition of human, drug-metabolizing cytochromes P450, *Anal. Biochem.*, 248 (1997) 188-190.

- [38] R.I. Geran, N.H. Greenberg, M.M. Macdonald, A.M. Schumacher, B.J. Abbott, Protocols for screening chemical agents and natural products against animal tumors and other biological systems, *Cancer Chemother. Rep.*, 3 (1972) 1-103.
- [39] Y. Zhao, X. Zhang, Y. Chen, S. Lu, Y. Peng, X. Wang, C. Guo, A. Zhou, J. Zhang, Y. Luo, Q. Shen, J. Ding, L. Meng, J. Zhang, Crystal structures of PI3K α complexed with PI-103 and its derivatives: New directions for inhibitors design, *ACS Med. Chem. Lett.*, 5 (2013) 138-142.
- [40] A. Zask, J.C. Verheijen, K. Curran, J. Kaplan, D.J. Richard, P. Nowak, D.J. Malwitz, N. Brooijmans, J. Bard, K. Svenson, J. Lucas, L. Toral-Barza, W.G. Zhang, I. Hollander, J.J. Gibbons, R.T. Abraham, S. Ayral-Kaloustian, T.S. Mansour, K. Yu, ATP-competitive inhibitors of the mammalian target of rapamycin: design and synthesis of highly potent and selective pyrazolopyrimidines, *J. Med. Chem.*, 52 (2009) 5013-5016.
- [41] Schrodinger Suite 2012, Glide version 5.8, Prime version 3.1, Desmond v3.7, Schrödinger, LLC, New York, NY, 2012.

TABLE CAPTIONS

- Table 1.** *In-vitro* PI3K- α inhibition and isoform-selectivity over other isoforms^a
- Table 2.** *In-vitro* cytotoxicity of 6-aryl substituted 4-(4-cyanomethyl)phenylamino quinazolines **9a-x** and **19** in a panel of cancer cells
- Table 3.** *In-vitro* cytotoxicity of 6-aryl substituted 4-(4-cyanomethyl)phenylamino quinazolines **9x** and **9u** in MCF-7 and normal cell lines
- Table 4.** *In-vivo* anticancer activity of compounds **9u** and **9x** in Ehrlich Ascites carcinoma (EAC) and Ehrlich Solid Tumor (EST) models

FIGURE / SCHEME CAPTIONS:

- Figure 1.** (A) Structures of pan-PI3K/mTOR inhibitor NVP-BEZ-235 (**1**)/ BAY 80-6946 (**8**), isoform-selective inhibitors idelalisib (**2**), NVP-BYL719 (**3**), GDC-032 (**4**) and INK1117 (**5**), AZD-8186 (**6**), AZD-6482 (**7**). (B) Structure-based design of 6-aryl substituted 4-(4-cyanomethyl)phenylamino quinazolines **9** as a potential isoform-selective PI3K- α inhibitors.
- Figure 2.** Interactions of compounds **9u** (a) and **9x** (b) with PI3K α
- Figure 3.** Western-blot analysis of compounds **9u** and **9x**. (a-b) the effect of compound **9u** on the expression of various isoforms of PI3K in MCF-7 cells. (c-d) the effect of compound **9x** on the expression of various isoforms of PI3K in PC-3 cells. Cells (2×10^6) were treated with the indicated concentrations of compounds **9u** and **9x**. Cells were lysed, and Western blot for different proteins was performed as described in biology protocols. β -Actin was used as internal control. *p-values/ <0.001 were considered significant.
- Scheme 1.** Synthesis of 6-aryl quinazolines **9a-x** and **19**. Reagents and conditions: (a) (i) Br₂, AcOH, 0 °C-rt (ii) dil.HCl, 100 °C, 55%; (b) NH₂CHO, 150 °C, 6 h, 70-76%; (c) POCl₃, 120 °C, 6 h, 74-82%; (d) Isopropanol, 80 °C, 3 h, 37-81%; (e) Pd(PPh₃)₄, 2M aqueous K₂CO₃, dioxane, 90 °C, 12 h, 43-81%.

Table 1. *In-vitro* PI3K- α inhibition and isoform-selectivity over other isoforms^a

Entry	% Inhibition of PI3K- α at 0.5 μ M	PI3K inhibition (IC ₅₀ in μ M)				Isoform-selectivity for α -isoform <i>versus</i> other isoforms		
		- α	- β	- γ	- δ	- β	- γ	- δ
9a	36.8	0.475	>10	6.95	>10	>21	14.6	>21
9b	17	nd	nd	nd	nd	nd	nd	nd
9c	1.3	nd	nd	nd	nd	nd	nd	nd
9d	44	0.270	>10	0.15	>10	>37	0.5	>37
9e	69.9	0.115	0.67	1.84	0.27	5.8	16	2.3
9f	38.1	0.451	>10	0.85	>10	>22.2	1.9	>22.2
9g	4.1	nd	nd	nd	nd	nd	nd	nd
9h	36.4	>10	>10	0.52	>10	1	-	1
9i	11	nd	nd	nd	nd	nd	nd	nd
9j	16.4	nd	nd	nd	nd	nd	nd	nd
9k	NI ^b	nd	nd	nd	nd	nd	nd	nd
9l	NI	nd	nd	nd	nd	nd	nd	nd
9m	20.3	nd	nd	nd	nd	nd	nd	nd
9n	8.2	nd	nd	nd	nd	nd	nd	nd
9o	33	0.342	>10	1.37	>10	>29.2	4	>29.2
9p	48.6	0.321	>10	0.19	>10	>31.1	0.6	>31.1
9q	29.8	nd	nd	nd	nd	nd	nd	nd
9r	2.7	nd	nd	nd	nd	nd	nd	nd
9s	1.5	nd	nd	nd	nd	nd	nd	nd
9t	NI	nd	nd	nd	nd	nd	nd	nd
9u	47.5	0.201	>10	0.75	>10	>49.7	3.7	>49.7
9v	NI	nd	nd	nd	nd	nd	nd	nd
9w	45.6	0.704	>10	0.36	>10	>14.2	0.5	>14.2
9x	48.8	0.150	>20	8.44	0.88	>133	56	5.9

19	NI ^c	47	19	40	55	nd	nd	nd
1	nd	0.004	0.076	0.007	0.005	19	17.5	1.25

^a all compounds were tested for mTOR inhibition at 1 μ M, however none of the compound was active.

^b NI, no inhibition at tested concentration; nd: not determined.

Table 2. *In-vitro* cytotoxicity of 6-aryl substituted 4-(4-cyanomethyl)phenylamino quinazolines **9a-x** and **19** in a panel of cancer cells

Entry	<i>In-vitro</i> cytotoxicity (GI ₅₀ in μ M)				
	HL-60	A375	MCF-7	Panc-1	PC-3
9a	23	38	14	38	26
9b	7	9	10	21	28
9c	42	39	91	90	21
9d	28	32	45	13	24
9e	24	28	15	36	37
9f	15	23	12	7	29
9g	36	32	>100	68	38
9h	16	27	11	32	34
9i	14	16	12	13	13
9j	32	24	23	40	27
9k	16	13	29	30	10
9l	16	30	26	33	17
9m	16	32	13	33	14
9n	25	31	16	48	22
9o	21	27	34	32	34
9p	27	24	34	33	7
9q	17	10	9	28	8
9r	14	14	8	24	13
9s	12	36	27	31	16
9t	31	34	34	33	18
9u	18	31	7	16	24
9v	44	89	32	90	23
9w	32	35	32	39	76
9x	10	12	12	9	9

19

47

19

40

55

34

ACCEPTED MANUSCRIPT

Table 3. *In-vitro* cytotoxicity of 6-aryl substituted 4-(4-cyanomethyl)phenylamino quinazolines **9x** and **9u** in MCF-7 and normal cell lines

Cell line	<i>In-vitro</i> cytotoxicity (GI ₅₀ in μ M)	
	9x	9u
MCF-7	7	12
fR2	>50	>50
HEK-293	>50	>50
hGF	>50	>50

Table 4. *In-vivo* anticancer activity of compounds **9u** and **9x** in Ehrlich Ascites carcinoma (EAC) and Ehrlich Solid Tumor (EST) models

Entry	EAC		EST	
	Dose (mg/kg, i/p)	% TGI (mortality)	Dose (mg/kg, i/p)	% TGI (mortality)
Control N.S. i/p	0.2 ml	0 (0/10)	0 0.2 ml	0 (0/10)
9u	25	62.01 (0/7)	15	34.33 (0/7)
			25	36.50 (0/7)
9x	70	25.79 (0/7)	nd	nd
5-FU	20	96.93 (0/7)	22	50.04 (0/7)

nd; not determined, 5-FU: 5-flurouracil.

FIGURES

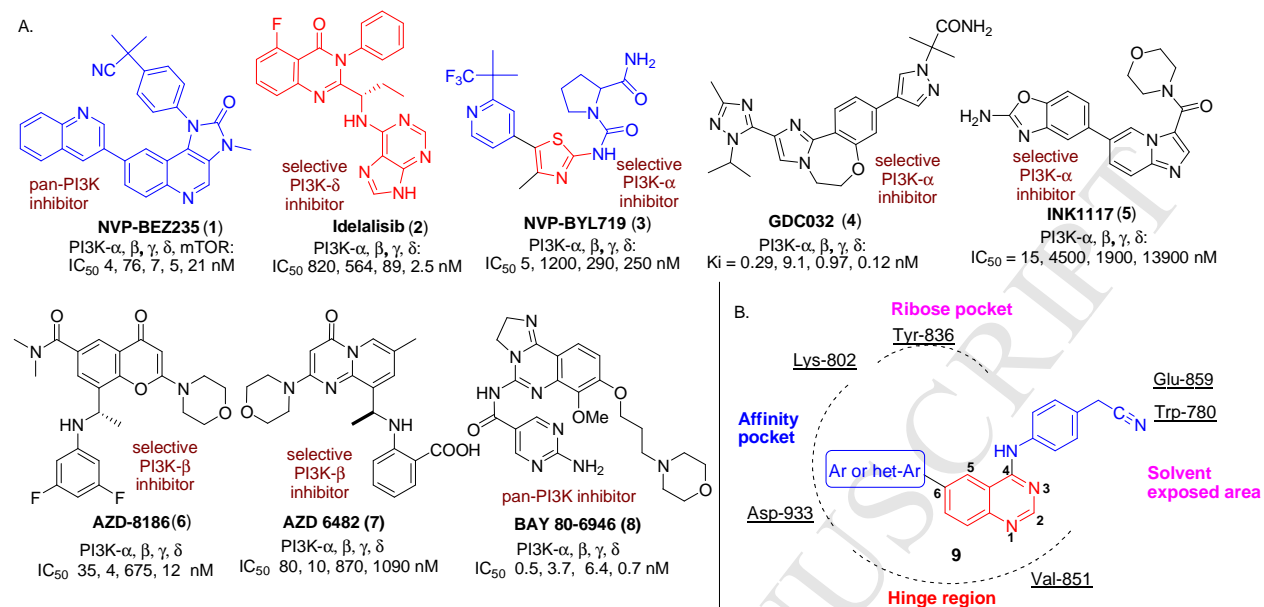


Figure 1.

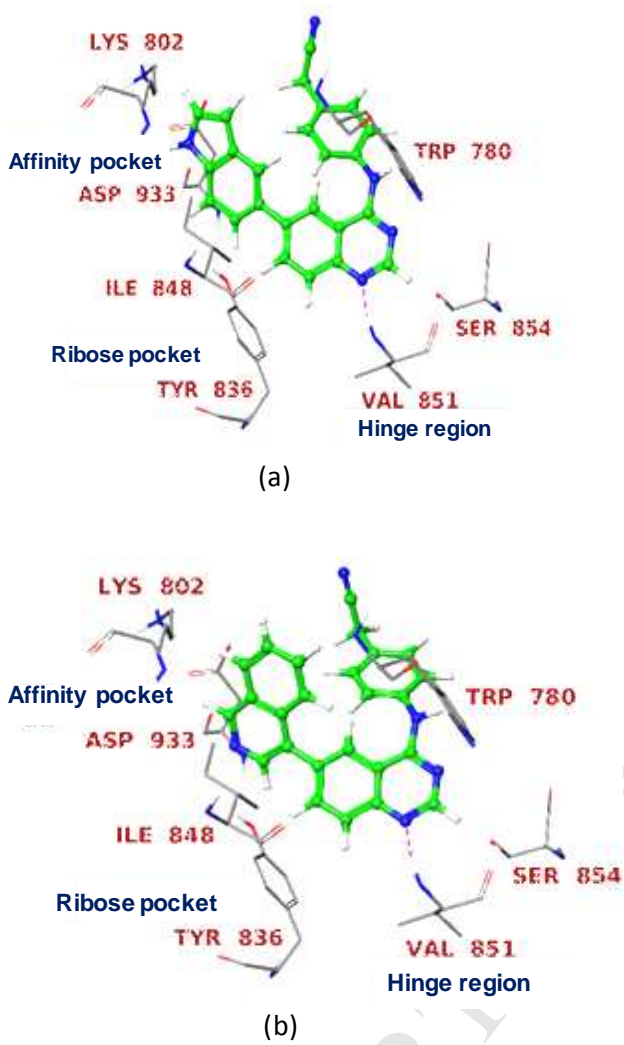


Figure 2.

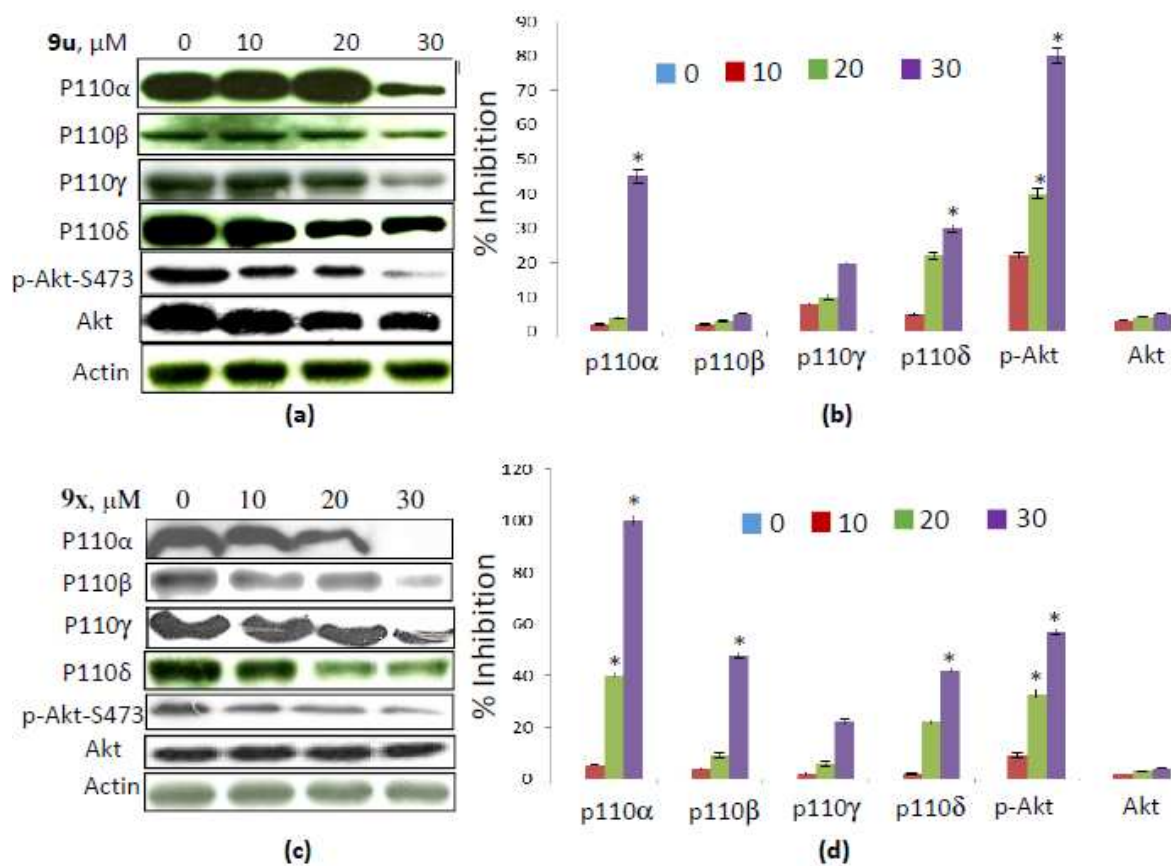
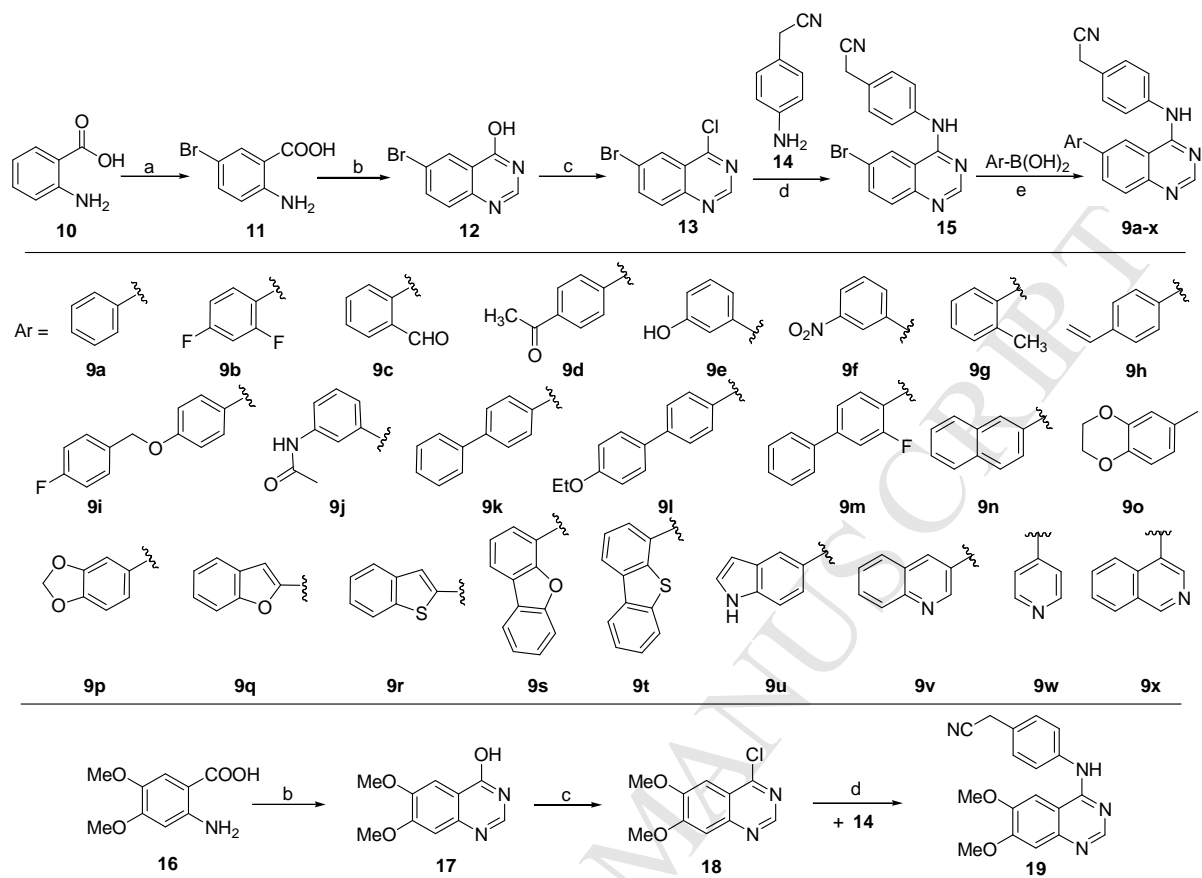


Figure 3.



Scheme 1.

Highlights

- 'Quinazoline' as a new chemotype for isoform-selective PI3K- α inhibition.
- Isoform-selectivity demonstrated at protein-expression level.
- These PI3K-alpha inhibitors showed inhibition of phospho-Akt.
- Quinazolines **9u** and **9x** showed promising cytotoxicity in MCF-7 cells.
- These were highly selective for cancer cells, and non-toxic to normal cells.
- Showed in-vivo activity in murine cancer models.